ESTUDO DA EFICIÊNCIA DO CHECKPOINT MITÓTICO NUMA LINHA CELULAR DE MEDULOBLASTOMA

MARIA JOANA ALMEIDA RODRIGUES BARBOSA

Dissertação de Mestrado em Bioquímica

Universidade do Porto

Faculdade de Ciências

uto de Ciências Biomédicas Abel Salazar

2009

ESTUDO DA EFICIÊNCIA DO CHECKPOINT MITÓTICO NUMA LINHA CELULAR DE MEDULOBLASTOMA

MARIA JOANA ALMEIDA RODRIGUES BARBOSA

Dissertação de Mestrado em Bioquímica

Universidade do Porto
Faculdade de Ciências
Instituto de Ciências Biomédicas Abel Salazar

2009

MARIA JOANA ALMEIDA RODRIGUES BARBOSA

ESTUDO DA EFICIÊNCIA DO CHECKPOINT MITÓTICO NUMA LINHA CELULAR DE MEDULOBLASTOMA

Dissertação de Candidatura ao grau de Mestre em Bioquímica da Universidade do Porto

Instituição de Acolhimento – Centro de Investigação em Ciências da Saúde (CICS), Instituto Superior de Ciências da Saúde – Norte (ISCS-N)/CESPU

Orientador – Doutor Hassan Bousbaa

Categoria – Professor Associado

Afiliação – Departamento de Ciências e CICS, ISCS-N/CESPU

Co-orientador – Doutora Roxana Moreira

Categoria – Professora Auxiliar

Afiliação – Departamento de Ciências e CICS, ISCS-N/CESPU

2009

Acknowledgements

Ao Prof. Doutor Hassan Bousbaa e à Prof.ª Doutora Roxana Moreira, por me terem aceite como sua mestranda, pela disponibilidade incondicional ao longo de todo o meu trabalho de mestrado, pela paciente revisão da presente tese e pelo exemplo dos seus percursos científicos, profissionais e pessoais.

À Prof.ª Doutora Odília Queirós, pelo acompanhamento próximo do curso dos meus trabalhos e pelas valiosas sugestões para a sua progressão.

À Dr.ª Olga Martinho e ao Prof. Doutor Rui Reis (ICVS, Universidade do Minho), pela cedência das linhas celulares Daoy e S462 e do extracto de RNA total de astrócitos.

À Juliana e à Ana Vanessa, com quem tenho a sorte de partilhar um percurso comum desde há muito, pela sua presença amiga, atenta e constante, pela sua boa-disposição, tolerância, solidariedade e gratuidade, bem como pelos seus exemplos de iniciativa e capacidade de trabalho.

À Kelly, pelo seu espírito activo, pela sua generosidade, boa-disposição e amizade, e pela forma como ilustra o conceito de trabalho em equipa.

Ao Daniel, à Nita, à Vânia, à Catarina e à Ana Rita, pela amizade, incentivo e afinidades que transcendem os tempos de faculdade.

À Rita e à Virgínia, pelos momentos calorosos passados dentro e fora do laboratório, que com a sua amizade e partilha de experiências e conhecimentos ilustram as potencialidades de uma equipa multidisciplinar.

À Vanessa, pelo companheirismo de uma vida e por tão bem saber ajudar-me a relativizar os obstáculos que se me vão deparando. Pelo genuíno e gratificante exemplo de vocação, gosto e dedicação pelo que se faz e por quem se faz.

Aos meus irmãos. À Marta, *for always leading my way*. Ao Eduardo, por ter sempre algo a ensinar-me e com que me fazer rir. A ambos agradeço o apoio incondicional, a partilha de interesses e o sentido de humor que tanto aprecio.

Aos meus pais, a quem devo a conquista de mais esta etapa, pela confiança que sempre depositaram em mim, pelas palavras de incentivo e carinho que sempre souberam dizer-me e pelo insubstituível exemplo de honestidade, persistência e trabalho.

Index

Abstract

Genetic instability constitutes the main cause of cancer development in man, with chromosome instability (CIN) being one of its forms and deriving from abnormalities in chromosome segregation during mitosis. In order to prevent CIN, cells possess a mechanism of control, the mitotic checkpoint, which consists of a signal transduction pathway activated to detect and repair eventual errors in chromosome segregation by delaying anaphase onset until all chromosomes are appropriately attached in a bipolar fashion to the mitotic spindle.

Medulloblastoma is the most frequent malignant central nervous system neoplasm of childhood. Most paediatric medulloblastomas have abnormal karyotypes, including aneuploidy. The present work aimed at detecting possible defects in mitotic checkpoint activity and the underlying molecular alterations in the Daoy medulloblastoma cell line. HeLa (cervical cancer) and S462 (Malignant Peripheral Nerve Sheath Tumour) cell lines were used as controls for the mitotic checkpoint efficiency.

Mitotic checkpoint competence was assessed through incubation with microtubule-disrupting nocodazole. Upon exposure to the drug, both HeLa and S462 cells accumulate in mitosis and eventually die as a response to microtubule depolymerisation, reflecting the efficiency of their mitotic checkpoint. Daoy cells, in turn, are capable of exiting mitosis and escaping from cell death in the presence of nocodazole, being able to survive even after prolonged incubation with the drug, an ability that is supported by their comparatively lower mitotic index. Chromosome spread analysis also reveals significant sister chromatid separation upon incubation with nocodazole, confirming that Daoy cells prematurely exit mitosis. Immunofluorescence analysis has shown that subcellular localisation of mitotic checkpoint proteins has no detectable changes in Daoy cells. However, Western blotting and quantitative Real-Time PCR assays denote alterations in their expression levels. In particular, BubR1, Bub3 and Mad2 are underexpressed, while there is Cdc20 and Chfr overexpression.

Alterations in these proteins' expression account for the observed mitotic checkpoint defects in Daoy cells and may act as aneuploidy promoters and participate in medulloblastoma's progression and/or malignancy.

Resumo

A instabilidade genética constitui a principal causa de desenvolvimento de cancro no Homem, sendo a instabilidade cromossómica, resultante de anomalias na segregação cromossómica ocorrida aquando da mitose, uma das suas formas. No sentido de evitarem a instabilidade cromossómica, as células dispõem de um mecanismo de controlo, o *checkpoint* mitótico, que consiste numa via de transdução de sinal activada para detectar e reparar eventuais erros na segregação cromossómica. Esta via actua atrasando o início da anafase até que todos os cromossomas se encontrem ligados de forma adequada e bipolar ao fuso mitótico.

Os meduloblastomas constituem as neoplasias malignas do sistema nervoso central mais frequentes em crianças. A maioria dos meduloblastomas pediátricos revela anormalidades cariotípicas, incluindo aneuploidia. O presente trabalho teve como objectivos a detecção de possíveis falhas na actividade do *checkpoint* mitótico e as alterações moleculares subjacentes na linha celular Daoy, derivada de meduloblastoma. As linhas celulares HeLa (cancro cervical) e S462 (*Malignant Peripheral Nerve Sheath Tumour*) foram utilizadas como controlos da eficiência do *checkpoint* mitótico.

A actividade do *checkpoint* mitótico foi avaliada através da incubação com nocodazole, uma droga despolimerizadora de microtúbulos. Após exposição à mesma, as células HeLa e S462 acumulam em mitose e eventualmente morrem como resposta à despolimerização dos microtúbulos, reflectindo a eficiência do seu *checkpoint* mitótico. Por sua vez, as células Daoy mostraram-se capazes de sair da mitose e de escapar à morte celular na presença de nocodazole, sobrevivendo mesmo após incubação prolongada, o que foi também corroborado pelo seu índice mitótico comparativamente menor. Ensaios de *chromosome spread* revelaram igualmente uma significativa percentagem de células com separação de cromátidas irmãs mediante incubação com nocodazole, confirmando que as células Daoy saem prematuramente da mitose. A análise por imunofluorescência revelou a ausência de alterações detectáveis na distribuição subcelular de proteínas do *checkpoint* mitótico. Contudo, ensaios de Western blotting e de Real-Time PCR quantitativo evidenciaram alterações nos seus níveis de expressão, demonstrando, mais concretamente, a sob-expressão de BubR1, Bub3 e Mad2, assim como a sobre-expressão de Cdc20 e de Chfr.

As alterações na expressão de proteínas do *checkpoint* mitótico justificam as falhas na sua actividade nas células Daoy, podendo constituir um mecanismo promotor de aneuploidia e contribuir para a progressão e/ou malignidade dos meduloblastomas.

Abbreviations

APC: Adenomatous Polyposis Coli
APC/C: Anaphase-Promoting Complex/Cyclosome
bp: base pairs
BRCA1: Breast Cancer 1
Bub: Budding uninhibited by benzimidazole
BubR1: Bub1-related protein
Cdc20: Cell-division-cycle 20 homologue
CDK: Cyclin-Dependent Kinase
cDNA: complementary Deoxyribonucleic Acid
CENP-E: Centromere Protein E
Chfr: Checkpoint with fork-head associated and ring finger
CIN: Chromosomal Instability
CO_2: Carbon Dioxide
DAPI: 4', 6-diamidino-2-phenylindole
D-MEM: Dulbecco's Modified Eagle Medium
DMSO: Dimethylsulfoxide
DNA: Deoxyribonucleic Acid
DTT: Dithiothreitol
ECL: Enhanced Chemiluminescence
EDTA: Etylenediaminetetracetic Acid
FBS: Foetal Bovine Serum
GAPDH: Glyceraldehyde-3-phosphate-dehydrogenase
HRP: Horseradish peroxidase
H_2O_2: Hydrogen Peroxide
Kbp: Kilo base pairs
kDa: kiloDaltons
M: molar (mol dm^{-3})
Mad: Mitotic arrest deficient
MAPK: Mitogen-Activated Protein Kinase
MCC: Mitotic Checkpoint Complex
µg: micrograms
µl: microlitres
µm: micrometres
µM: micromolar
ml: millilitres
mm: millimetres
mM: millimolar
MI: Mitotic Index
MPNST: Malignant Peripheral Nerve Sheath Tumour
Mps1: Monopolar spindle 1
MTOC: Microtubule-organizing centre
nm: nanometres
nM: nanomolar
OD: Optical Density
PBS: Phosphate-Buffered Saline
PBST: Phosphate-Buffered Saline and Tween-20
PCR: Polymerase Chain Reaction
PFA: Paraformaldehyde
Plk1: Polo-like kinase 1
PMSF: Phenylmethylsulfonyl Fluoride
PTEN: Phosphatase and Tensin Homologue
RB1: Retinoblastoma 1
RNA: Ribonucleic Acid
RNAi: RNA interference
RNase: Ribonuclease
RZZ: ROD-ZW10-ZWILCH complex
rpm: rotations per minute
SAC: Spindle Assembly Checkpoint
SCS: Sister Chromatid Separation
SD: Standard Deviation

SDS: Sodium Dodecyl Sulfate

SDS-PAGE: Sodium Dodecyl Sulfate-Polyacrylamide Gel Electrophoresis

Shh-Ptch: Sonic hedgehog-Patched pathway

TBS: Tris-Buffered Saline

TBST: Tris-Buffered Saline and Tween-20

TP53: Tumour Protein p53

Tris: Tris-(hydroxymethyl)aminemethane

ZW10: Zeste White 10

1. INTRODUCTION

1.1 The cell cycle

The cell cycle is a ubiquitous and complex process of major importance in the growth and proliferation of cells, development of all living organisms, regulation of DNA damage repair and tissue regeneration (Schafer, 1998). It is a sequential phenomenon, orchestrated and controlled by numerous regulatory proteins that direct the cell through a specific series of highly coordinated events in a generally invariant order (Schafer, 1998; Clarke and Giménez-Abián, 2000). Nonetheless, cell cycle-related deregulations have been shown to be associated with a number of pathologies, particularly with cancer (Garrett, 2001; Vermeulen *et al.*, 2003; Kops *et al.*, 2005; Bharadwaj and Yu, 2004). In particular, aneuploidy – an abnormal chromosomal content – has been observed in a variety of tumour cells, suggesting that defects in the mechanisms that control cell division and chromosome segregation may be involved in tumorigenesis.

The somatic cell cycle may be defined as the period comprised between two mitotic divisions. It may be divided into two main stages: the M phase, which refers to the period where division actually occurs, and the interphase, which corresponds to the time from the end of one mitotic division until the start of the next. In order to be able to divide and originate two new identical daughter cells, each of them bearing a diploid set of chromosomes, a eukaryotic somatic cell must double its size and its contents. In reality, the doubling of its size is a continuous process, deriving from constant transcription and translation of genes encoding for the proteins that are needed to a specific phenotype. However, DNA replication is confined to a particular phase of the cycle. Interphase encompasses the G1, S and G2 periods, which were actually identified accordingly with the timing of DNA synthesis. In G1, there is RNA and protein synthesis, but no DNA replication, with no apparent changes in cell morphology. The S phase, in turn, lasts from the beginning of DNA replication until it is all replicated. In this step, the total DNA content increases from the diploid value $2n$ to the fully replicated value of $4n$ and the cell increases noticeably in size, in part because of proteins that accumulate to match DNA synthesis. G2 comprises the period between the S phase and mitosis, in which the cell possesses two complete sets of chromosomes. Thus, G1 and G2 stand for the 'gap' periods in which there is no DNA replication, whilst the S phase refers to the synthetic

period when DNA is replicated. Virtually, all synthetic activities are suspended during mitosis (Vermeulen *et al.*, 2003; Lewin, 2004).

It must be stated that, when in G1, cells may alternatively withdraw from the cycle into the G0 phase, a quiescence state, for an indefinite period of time (e.g., when nutrient supply is not favourable); conversely, they may reactivate and re-enter the cell cycle in G1 phase at any time (**fig. 1.1**).

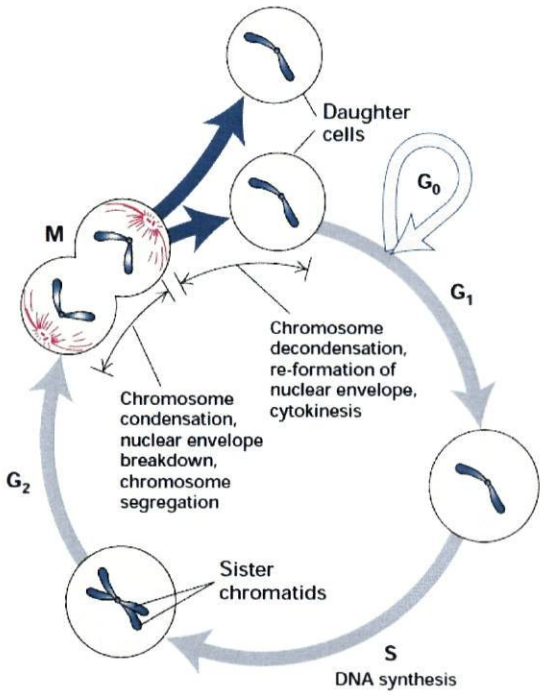

Fig. 1.1: The eukaryotic cell cycle. Interphase comprises G1, S and G2 phases. In G1 (6-12 hours) and in G2 (3-4 hours), there is RNA and protein synthesis; in S phase (6-8 hours), there is also DNA replication. One cell cycle is separated from the next by mitosis, the M phase (1 hour), in which karyocinesis (nuclear division) and cytokinesis (cell division) yield two identical daughter cells. Terminally differentiated cells may alternatively enter a quiescent phase (G0) for an indefinite period of time (Lodish *et al.*, 2000).

Successful division is dependent on the coordinated duplication and segregation of all cell components. This, in turn, is under the control of a family of highly regulated protein kinases known as cyclin-dependent kinases (Cdks). As their name implies, their activity requires the binding to a cyclin subunit (McGowan, 2003; Murray, 2004). Cyclins were originally characterized as proteins whose levels changed periodically during the cell cycle; in fact, Cdk most fundamental level of control is cyclin intermittent expression (**fig. 1.2**) (Schafer, 1998; McGowan, 2003; Murray, 2004; Sullivan and Morgan, 2007).

The first cyclin to be expressed following the quiescence state is cyclin D, which assembles with Cdk4 and Cdk6 (**fig. 1.2**). This complex enters the nucleus and promotes phosphorylation of the retinoblastoma protein (Rb) and the related pocket proteins p107 and p130. Rb phosphorylation stimulates the activation of the E2F family of transcription factors and induces the transcription of fundamental proteins for G1 and S phase (Schafer, 1998; McGowan, 2003). The same mitogenic stimuli that promote cyclin D production also promote cyclin E expression, as well as of two cyclin-dependent kinase inhibitors, $p21^{cip1}$ and $p27^{kip1}$ (Sherr and Roberts, 1999; Egozi *et al.*, 2007). These latter proteins are necessary for the efficient assembly and nuclear import of active cyclin D-Cdk4 complexes and delay activation of cyclin E-Cdk2 in early G1 (McGowan, 2003).

The activation of cyclin E-Cdk2 is concomitant with the beginning of DNA replication. Cyclin E-Cdk2 phosphorylates the inhibitor protein p27, facilitating its ubiquitination and subsequent degradation (Sherr and Roberts, 1999; Egozi *et al.*, 2007). Cyclin E-Cdk2 also autophosphorylates on cyclin E, similarly targeting it to degradation. For this reason, the kinase complex is said to be both self-activating and self-limiting (Schafer, 1998; McGowan, 2003).

Initiation and completion of DNA replication is also dependent on another complex, cyclin A-Cdk2 (Cuomo *et al.*, 2008). Cyclin A expression follows that of cyclin E, at the G1-S boundary. Both cyclin A-Cdk2 and cyclin E-Cdk2 are crucial to assure that DNA replication occurs only once per cycle. Moreover, cyclin A-Cdk2 increases transcription of histones and other genes, ensuring the efficient accomplishment of S phase by furnishing the material required for replication (McGowan, 2003).

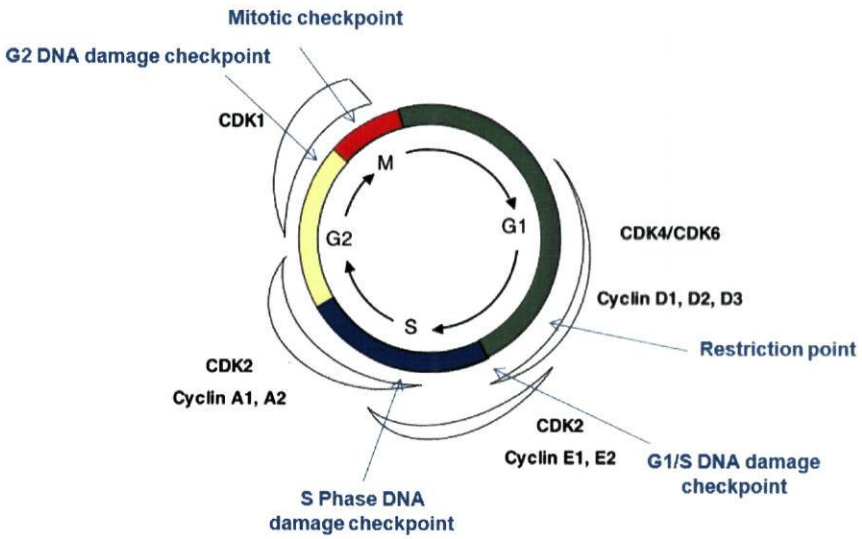

Fig. 1.2: Cell cycle regulation by Cdk-cyclin complexes. The approximate time of activity of the different Cdk-cyclin complexes throughout the cell cycle, based on studies with mammalian cells, is depicted. Shapes outside the cycle reflect increases and decreases of the corresponding Cdk-cyclin activities. Cell cycle checkpoints are also represented (adapted from Garrett, 2001; van den Heuvel, 2005).

The profound morphological changes that accompany mitosis are under the regulation of Cdk1(Cdc2) in association with cyclin A and cyclin B. Expression of cyclin B lags behind that of cyclin A, peaking late in S phase and remaining high during G2 and mitosis. Cyclin B-Cdk1 is largely maintained in a phosphorylated inactive state, and its posterior dephosphorylation and activation coincides with the morphological alterations that are typical of mitosis (McGowan, 2003). It is known that Cdk1, in association with a second cyclin B subunit – cyclin B2 –, plays a role in the division of single-copy organelles such as the endoplasmic reticulum, making sure that cell division occurs in a way that

supplies sufficient amounts of these organelles to each daughter cell, so that they can be rebuilt. Multi-copy organelles (e.g., mitochondria) are homogeneously distributed in the cytoplasm so that each daughter cell can inherit roughly the same amount of them (McGowan, 2003).

When cell cycle proteins have entirely performed their function, they must be degraded so that the events they elicited do not reoccur improperly. Ubiquitin-mediated degradation is the main pathway by which they are eliminated (Murray, 2004). Cyclins are targeted for ubiquitination by their PEST sequences, protein motifs rich in proline (P), glutamate (E), serine (S) and threonine (T) (Schafer, 1998). Protein tagging with ubiquitin residues signalises it to degradation by the 26S proteasome, a multisubunit cellular complex that is specialised in protein unfolding and proteolysis (Schafer, 1998).

1.1.1 Mitosis

Following interphase, cells enter mitosis, which, though a short-termed phase when considering the temporal context of the whole cell cycle, is remarkably important for cell division and normal proliferation since it ensures accurate segregation of genetic material into the two daughter nuclei. It is traditionally subdivided into five stages: prophase, prometaphase, metaphase, anaphase and telophase (**fig. 1.3**) (Nigg, 2001; McGowan, 2003; Lewin, 2004; Kops *et al.*, 2005).

At prophase, chromatin condensates, originating recognizable chromosomes. Until this phase, it was a compact mass with no visible change in its condensation state. Previously duplicated centrosomes separate and define the future poles of the mitotic spindle (Compton, 2000; Nigg, 2001; McGowan, 2003). In turn, numerous highly dynamic microtubules nucleate from centrosomes (Lewin, 2004; Doxsey *et al.*, 2005; Kops *et al.*, 2005). This is the reason why centrosomes are also known as microtubule organizing centres (MTOCs) (Crasta *et al.*, 2008; Kwon *et al.*, 2008).

At prometaphase, the nuclear envelope breaks down and the consequently dispersed chromosomes attach, through their kinetochores, to microtubules of the mitotic spindle through a 'search and capture' process (Gadde and Heald, 2004; Odde, 2005; Pinsky and Biggins, 2005; Yang *et al.*, 2008). The Golgi apparatus and the endoplasmic reticulum also break down into small membrane vesicles in this stage (Nigg, 2001; McGowan, 2003; Lewin, 2004; Kops *et al.*, 2005).

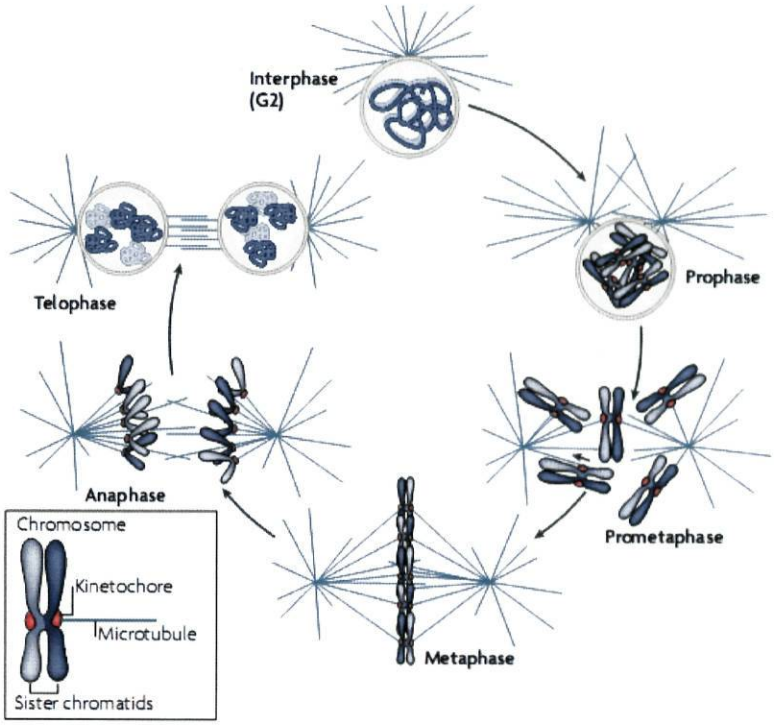

Fig. 1.3: The five stages of mitosis. Mitosis comprises orderly sequenced events. Nuclear envelope breakdown, chromosome condensation and centrosome separation take place at prophase, while in prometaphase chromosomes are captured by microtubules growing from the separated centrosomes and start to congress. At metaphase, all chromosomes are aligned at the equatorial plate. Upon chromatid separation and spindle pole elongation, occurring at anaphase, two daughter cells are originated at telophase, prior to cytokinesis. Then, cells return to interphase (Cheeseman and Desai, 2008).

At metaphase, all chromosomes have undergone proper bipolar attachment and alignment in the metaphase plate. Sister chromatid cohesion is then suddenly lost (**section 1.3.1.1**) and anaphase is initiated, comprising spindle elongation and consequent separation of sister chromatids. In the end of anaphase, the plasma membrane starts to evidence a certain degree of invagination around the spindle midzone, the contractile ring. Some authors distinguish between anaphase A and anaphase B, considering that the former is characterized by chromosome migration towards the poles and that, in the latter, further separation of the poles towards the cell cortex occurs (Nigg, 2001). Telophase is characterized by the progression of the contractile ring, which is composed of actomyosin fibers that extend around the equator of the dividing cell and then pinch inward until they contact a group of microtubules that run between the poles, giving rise to a structure connecting the future two daughter cells – the midbody. This structure is dissociated, ultimately leading to cytoplasm partitioning and to the formation of two new daughter cells, in a process called cytokinesis. In the meanwhile, chromatin has decondensed and the nuclear envelope is completely reconstituted around

the two daughter groups of chromosomes (Nigg, 2001; McGowan, 2003; Lewin, 2004; Kops *et al.*, 2005).

1.2 Kinetochore and microtubule structure and function

Genetic integrity maintenance is ensured by proper chromosome segregation during mitosis, which takes place on a bipolar spindle-shaped structure composed of microtubules. These interact with chromosomes through specialised complexes, the kinetochores, which are located in the centromeres, the sites of primary constriction of condensed chromosomes (Chan *et al.*, 2005; Tanaka and Desai, 2007; Cheeseman and Desai, 2008).

In effect, kinetochores constitute the macromolecular structures assembled on opposite sides of the centromere that form the interface between the chromosomes and the microtubules of the mitotic spindle, therefore playing a crucial role during mitosis (Chan *et al.*, 2005; Cheeseman and Desai, 2008). Kinetochores comprise several highly conserved subcomplexes whose functions include attachment of chromosomes to the spindle microtubules, monitoring these attachments – and, if defects are detected, initiating a signalling checkpoint pathway to prevent cell cycle progression –, kinetochore assembly and specification (that is, determining where on the chromosome will the kinetochore be assembled), and participating in chromosome movement along the spindle (Cheeseman and Desai, 2008).

Microtubules, in turn, are 25-nm diameter hollow polymers, comprised of 12-15 protofilaments that are formed by head-to-tail association of α/β-tubulin dimers. They alternate between phases of growth and shrinkage, a phenomenon referred to as 'dynamic instability'. Because tubulin dimers have a fixed orientation, the microtubule lattice is polar, influencing movements along the spindle (Maiato *et al.*, 2004; Cheeseman and Desai, 2008).

The structure of animal kinetochores may be described as a trilaminar stack of plates (**fig. 1.4**). The inner kinetochore is composed of repetitive DNA sequences and assembles into a specialized highly folded form of heterochromatin, containing nucleosomes with at least one specialised histone and auxiliary proteins, which persists all cell cycle. This kinetochore-adjacent single inner plate is thus a very ordered, modular structure (Maiato *et al.*, 2004). On the surface of the chromosome, there is a proteinaceous outer plate whose dynamic components assemble and function only during mitosis, more specifically at about the time of nuclear envelope breakdown (Maiato *et al.*, 2004). This outer plate displays about 15 to 20 end-on attachment sites for the plus ends

of microtubules (called kinetochore microtubules, kMTs) and is 50-60 nm-thick (Cheeseman and Desai, 2008). The outermost regions of the kinetochore constitute a fibrous corona, which is composed of several resident and transient components that are responsible for microtubule attachment and behaviour and for spindle checkpoint activity (Maiato *et al.*, 2004; Chan *et al.*, 2005). In cultured mammalian cells, duplicated kinetochores belonging to sister chromatids separate from one another during mid-late G2. Upon nuclear envelope breakdown, they acquire a mature laminar structure, in a process that depends on inner plate elements (Maiato *et al.*, 2004). The central kinetochore is the region comprised between inner and outer plates; it seems to be less dense than its neighbours and its protein composition has not been determined yet (Chan *et al.*, 2005; Cheeseman and Desai, 2008).

As far as kinetochore protein composition and interactions are concerned, it should be stated that they constitute a very broad subject that is continuously being updated. In humans, about 80 kinetochore proteins are known today (Cheeseman and Desai, 2008). Nevertheless, many components remain to be unravelled and the interdependencies established so far may suffer from slight changes. **Fig. 1.4** depicts some of the most important kinetochore protein components and their respective functions in the cell cycle (see Maiato *et al.*, 2004 for a review).

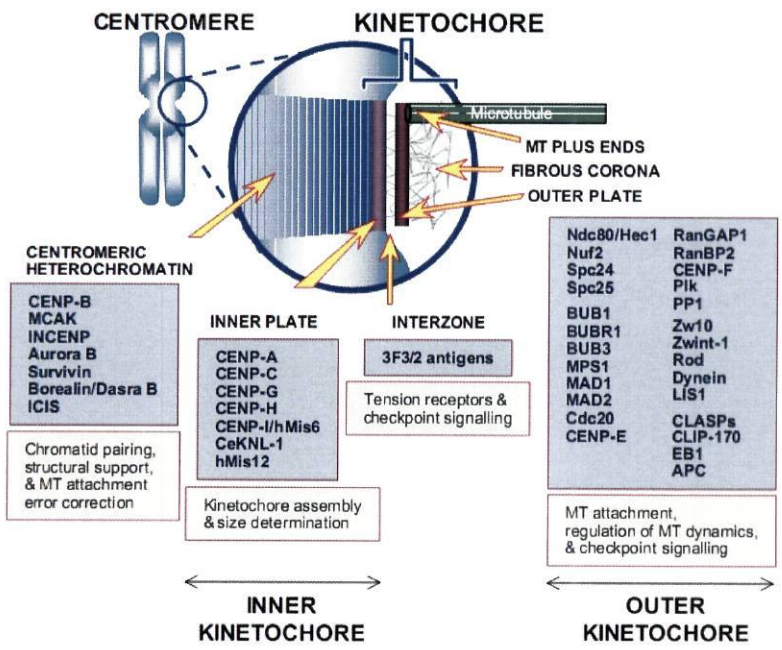

Fig. 1.4: Animal kinetochore organization. Some of kinetochore protein constituents, as well as their localisation and main functions are depicted. MT: microtubules (Maiato *et al.*, 2004).

Upon nuclear envelope breakdown, at prophase-to-prometaphase transition, usually microtubules become mono-oriented by one (monotelic attachment) or both (syntelic attachment) sister kinetochores. However, chromosome bi-orientation is required for accurate chromosome segregation, implying that one sister kinetochore must be bound to microtubules irradiating from solely one pole, whilst the other must be attached

to microtubules solely from the opposite pole. In other words, an amphitelic attachment must be achieved. Merotelic attachments, in turn, occur when one or both of the sister kinetochores are attached to microtubules from opposite poles (**fig. 1.5**) (Hauf and Watanabe, 2004; Maiato *et al.*, 2004; Musacchio and Salmon, 2007). Because it still originates tension, this situation is not detected by the spindle assembly checkpoint; instead, it is corrected by Aurora B/Ipl1 (Musacchio and Salmon, 2007).

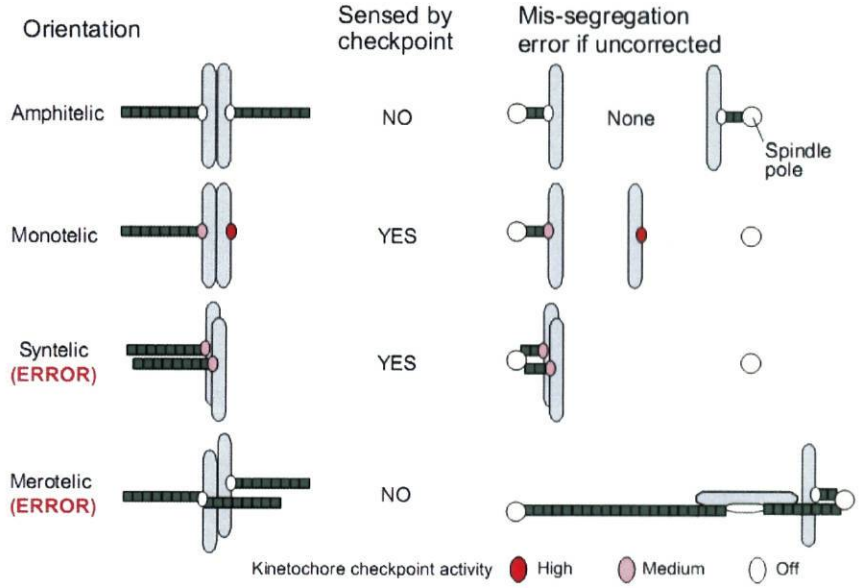

Fig. 1.5: Schematic representation of the most common kinetochore attachment errors. The corresponding extent of checkpoint activation and their consequences if they are not repaired before anaphase onset are represented. In an amphitelic attachment, sister kinetochores are attached to opposite poles. In a monotelic attachment, only one of the sister kinetochores is attached to one pole, while in a syntelic attachment both sister kinetochores are attached to the same pole. Finally, if there is one sister kinetochore attached to both poles, the attachment is considered to be merotelic. In monotelic and syntelic attachments, sister kinetochores are mono-oriented, while in amphitelic and in merotelic attachments, they are said to be bi-oriented (Maiato *et al.*, 2004).

1.3 Cell cycle checkpoints

The orderly progress through the cell cycle is assured by specific 'checkpoints' – control loops that make the initiation of each next event dependent on the proper accomplishment of the previous, being commonly defined as mechanisms that establish a dependence relationship between two cellular processes that are biochemically unrelated (Schafer, 1998; Clarke and Giménez-Abián, 2000). In other words, these checkpoints confirm cells' ability and readiness to proceed to a new stage, being superimposed on the cell cycle and acting directly on the regulatory molecules that control progression through it (Lewin, 2004). A checkpoint is made up of three components that act sequentially. The first component to operate is a sensor mechanism that detects incorrect or incomplete cell

cycle events, triggering a signalling pathway, the second component, which may culminate in the activation of an effector (the third and last component). This ultimate target promotes cell cycle arrest until the error is solved (Garrett, 2001).

In effect, four control points must be highlighted: DNA damage checkpoints occurring at G1/S, S and G2/M and the mitotic checkpoint (**fig. 1.2**). DNA damage is checked at every stage of the cycle, but especially at G1/S and G2/M transitions. At S phase, the cell verifies DNA integrity and the completion of its replication, which is a prerequisite for the division of probably all somatic eukaryotic cells. The G2/M checkpoint assures that every DNA sequence has been replicated totally and only once and that the cell does not begin mitosis until replication is completed (Kaufmann and Paules, 1996; Garrett, 2001).

The spindle checkpoint ensures the assembly of a functional mitotic spindle and inspects kinetochore attachments to microtubules, which is mentioned in greater detail in **section 1.3.1.1** (Garrett, 2001; Lewin, 2004). In case of functional DNA damage and/or spindle assembly checkpoints, the cell is able to correct the errors or, if they are too extensive or irremediable, it may undergo apoptosis, senescence, or mitotic catastrophe, for instance (Schmit and Ahmad, 2007).

Chfr (Checkpoint with Forkhead-associated and RING finger domains), reported as an early mitotic checkpoint protein, is an E3 ubiquitin ligase responsible for targeting proteins such as Plk1 and Aurora A for degradation (Kang *et al.*, 2002; Privette and Petty, 2008). In case of mitotic stress (for instance, in case of drug-induced microtubule depolymerisation), it has been shown to act in late G2, to delay prophase and entry into metaphase by inhibiting chromosome condensation, nuclear envelope breakdown and by excluding cyclin B1/Cdk1 from the nucleus (Scolnick and Halazonetis, 2000; Chaturvedi *et al.*, 2002; Gong, 2004; Loring *et al.*, 2008; Privette and Petty, 2008). Other studies support its role as a potent tumour suppressor and its importance, later in mitosis, for the control of centrosome separation, mitotic spindle formation, chromosome segregation, and mitotic spindle assembly checkpoint (Scolnick and Halazonetis, 2000; Privette *et al.*, 2007; Privette and Petty, 2008). In effect, Chfr was found to be required for proper BubR1 and Mad2 localization to the kinetochores and for Mad2/Cdc20 complex formation (**section 1.3.1**) (Privette *et al.*, 2007; Privette *et al.*, 2008). Several cancer cell lines – namely from lung, colon and esophageal neoplasms – display Chfr gene down-regulation or methylation-induced inactivation (Corn *et al.*, 2003; Toyota *et al.*, 2003), which correlate with tumour higher invasiveness and aneuploidy (Privette *et al.*, 2007; Loring *et al.*, 2008; Privette *et al.*, 2008). Chfr is thus implied as a regulator of genomic stability (Privette and Petty, 2008).

1.3.1 The spindle assembly checkpoint

The spindle assembly checkpoint (SAC) is a constitutive surveillance mechanism in eukaryotic dividing cells that prevents chromosome mis-segregation by delaying the metaphase-to-anaphase transition until all chromosomes are correctly connected to the microtubule network, bi-oriented and aligned at the metaphase plate (Rieder *et al.*, 1994; May and Hardwick, 2006; Logarinho and Bousbaa, 2008). It represents the primary cell-cycle control mechanism in mitosis, being activated immediately after mitosis or meiosis entrance, every cell cycle (Kops *et al.*, 2005). Regular functioning of this complex signalling cascade is the main responsible for the even partition of the genetic material into the two daughter cells and for the effective reduction of the error rate occurring during cell division.

Ever since attention has been drawn to the role of SAC, a set of proteins have been proven to be tightly associated with it and crucial to its functions (**table 1.1**). These 'core checkpoint proteins' comprise members of the Mad (Mitotic arrest deficient, Mad1-3) and Bub (Budding uninhibited by benzimidazole, Bub1-3) families, which have been initially identified by yeast mutagenesis screens for mutants unable to survive a temporary exposure to microtubule toxins nocodazole and benzimidazole (Earnshaw and Mackay, 1994; Bharadwaj and Yu, 2004). Mps1 (monopolar spindle 1) protein was also shown to play a relevant role in the spindle checkpoint, besides its initially identified function as a requirement for the proper assembly of bipolar spindles (Wang and Burke, 1995; Bharadwaj and Yu, 2004; Winey and Huneycutt, 2002). Subsequently, homologues for these proteins have been identified in higher organisms (including mammals) (Bharadwaj and Yu, 2004).

These proteins have been proven to share a high degree of both sequence and functional homology with their yeast counterparts, as functional disruption studies through dominant-negative mutants, antibody injection or RNA interference (RNAi) completely compromised the spindle checkpoint activity, causing chromosome mis-segregation, aneuploidy and mitotic arrest inability in the presence of microtubule poisons such as nocodazole and taxol (Bharadwaj and Yu, 2004).

Protein	Characteristics		Binding Partners	Comments
	Molecular weight (kDa)	Other		
Bub1	122	serine / threonine kinase	Bub3	Inhibits Cdc20 by phosphorylation. Required for recruiting other checkpoint proteins differs depending on system. Kinase activity is not required for checkpoint arrest.
BubR1	120	serine / threonine kinase	CENP-E, Bub3, Cdc20	Part of APC/C inhibitory complex. Directly binds to Cdc20 and inhibits APC/C activity. Interacts with Mad2 and Cdc20 to form the MCC. C-terminal kinase domain of BubR1 is activated by CENP-E. Yeast Mad3, the functional equivalent of BubR1, lacks the kinase domain, which is not required for the checkpoint.
Bub3	37	structure determined: 7-bladed propeller of WD40 repeats	Bub1, BubR1	Part of APC/C inhibitory complex. Localizes Bub1 and BubR1 to KTs.
Mad1	83	coiled coil	Mad2	Directly recruits Mad2 to unattached KTs. Localizes Mad2 to the NP in interphase; function at the NP is unknown. Binds to Bub1 and Bub3 upon checkpoint activation in budding yeast.
Mad2	23	structure determined	Mad1, Cdc20, CMT2/p31^{comet}	Part of APC/C inhibitory complex. Directly binds to Cdc20 and inhibits APC/C activity. Occurs in two conformations ('closed' C-Mad2 on binding Mad1 or Cdc20, or 'open' O-Mad2 when unbound); interacts with Cdc20 and BubR1/Mad3 to form the MCC.
Mps1	97	dual-specificity kinase	Unknown	Phosphorylates Mad1 *in vitro*. Excess activates the checkpoint. Required for recruitment of Mad1, Mad2 and CENP-E to the kinetochore. Required for spindle pole body duplication.
CENP-E	312	plus-end directed microtubule motor	BubR1	Binds to BubR1; stimulates BubR1 kinase activity. Required for capture and stabilization of microtubules at the kinetochore. Only found in higher eukaryotes.
ZW10	89	none identified	ROD, Zwilch	Part of complex that recruits the Mad1/Mad2 heterodimer to unattached KTs.
ROD	251	none identified	ZW10, Zwilch	Part of complex that recruits the Mad1/Mad2 heterodimer to unattached KTs.
Zwilch	67	none identified	ROD, ZW10	Part of complex that recruits the Mad1/Mad2 heterodimer to unattached KTs.

Table 1.1: Mitotic checkpoint core and related proteins/complexes. Most significant properties, interactions and functions are emphasized. KTs: kinetochores; MCC: Mitotic Checkpoint Complex; NP: Nuclear Periphery (adapted from Lew and Burke, 2003; Chan *et al.*, 2005; Kops *et al.*, 2005; May and Hardwick, 2006).

Other SAC proteins include the Aurora kinase B, the plus-end directed kinesin motor protein CENP-E (Centromere protein E), MAPK (mitogen-activated protein kinase) (Kops *et al.*, 2005), as well as the minus-end directed motor dynein and the proteins with which it interacts – dynactin, CLIP170 and LIS1, and the RZZ (ROD-ZW10-ZWILCH) complex (Karess, 2005; Schmidt and Medema, 2006; Logarinho and Bousbaa, 2008). The fact that these proteins do not have yeast orthologues suggests a more complex regulation of mitosis in higher eukaryotes, in which they are actually required for normal mitotic timing, as opposite to what happens in yeast (Taylor, 2004; May and Hardwick, 2006). A description of some proteins involved in SAC activity is provided on **table 1.1**.

In addition to the proteins that have been mentioned so far, recent works have shed light on other components that seem to play a role in checkpoint signalling in metazoans. That is the case of the microtubule-affinity regulating kinase (MARK)-family kinase TAO1, Polo-like kinase-1-interacting checkpoint helicase (PICH), and the deubiquitylase USP44 (involved in the regulation of the cytosolic ubiquitination status of Cdc20). Dynein at kinetochores has been suggested to function in checkpoint inactivation, while a protein named Spindly was recently associated with dynein recruitment and checkpoint silencing (Cheeseman and Desai, 2008).

1.3.1.1 The spindle assembly checkpoint acts by preventing anaphase onset

Sister chromatids are held together by a complex of cohesin proteins, formed in S phase, which acts as a sort of 'glue' (through DNA cross-linking) (Marangos and Carroll, 2008). It is located at diverse sites along a pair of sister chromatids, appearing to be centrally localised between the chromatids (Lewin, 2004). Anaphase onset implies degradation of one of cohesin's subunits, Scc1, which is promoted by the proteolytic activity of separase (Nasmyth, 2005). Separase, in turn, is normally kept inactive by securin. When all chromosomes are correctly attached to microtubules, SAC requirements are fulfilled and securin is then ubiquitinated by the anaphase promoting complex/cyclosome (APC/C), a multi-subunit E3 ubiquitin ligase (Morgan, 1999; Reddy *et al.*, 2007; Stegmeier *et al.*, 2007; Logarinho *et al.*, 2008). Securin ubiquitination targets it to degradation by the 26S proteasome. Separase is then activated and Scc1, an important component of the cohesin complex, is cleaved, no longer holding the chromatids together. Thus, they become free to segregate on the spindle, initiating anaphase (**fig. 1.6**) (Morgan, 1999; Bharadwaj and Yu, 2004; Lewin, 2004; Nasmyth, 2005). Degradation of cyclin B1, another important mitotic protein, is also accomplished through APC/C-mediated ubiquitination, leading to the inactivation of cyclin-dependent

kinase 1 (Cdk1). Cyclin B1 destruction makes it possible to reverse all the phosphorylations that elicited mitosis, thus propitiating mitotic exit (Lewin, 2004; May and Hardwick, 2006; Schmidt and Medema, 2006; Logarinho and Bousbaa, 2008).

Securin ubiquitination by APC/C is dependent on the binding of the WD40-repeat-containing cell-division-cycle 20 homologue (Cdc20) protein, which is responsible for substrate recruitment to APC/C. In fact, the complex between APC/C and Cdc20 (APC/C^{Cdc20}) is the most downstream target of the spindle assembly checkpoint (Bharadwaj and Yu, 2004). Cdc20 is actually necessary for the APC to degrade securin, which, as already mentioned, controls metaphase-to-anaphase transition (Lewin, 2004). Ubiquitin ligase activity is reinforced by the phosphorylation of Cdc20 and APC core components by cyclin B-Cdk1 (McGowan, 2003). In turn, Mad2, the protein that binds and sequesters Cdc20, is critical for SAC functioning. It can adopt either an open conformation (O-Mad2) or a closed form (C-Mad2). The latter is a more potent inhibitor of APC/C *in vitro* given its higher affinity for Cdc20, and Mad2 binding to Mad1 is thought to promote conformational switch to the closed form (**fig. 1.6**) (Chan *et al.*, 2005; Musacchio and Salmon, 2008). In effect, it was proven that Mad2 binding to Mad1 in a 2:2 tetramer is required for *in vivo* Mad2:Cdc20 complexation (Mapelli *et al.*, 2006).

Cdh1, like Cdc20, has also been reported as an APC/C regulatory protein, interacting and presenting certain substrates to APC/C for ubiquitination (May and Hardwick, 2006; Crasta *et al.*, 2008). It is also required for the APC/C to degrade cyclin B, therefore being a prerequisite for the cell to exit mitosis (Lewin, 2004). APC-Cdh1 activity early in G1 verifies that all mitotic proteins are destroyed prior to the initiation of DNA replication in the next cell cycle (McGowan, 2003; Sullivan and Morgan, 2007).

Once the nuclear envelope is broken-down, checkpoint proteins are recruited to the outer kinetochore surface of all unattached chromosomes. A single unattached or mis-attached kinetochore emits an inhibitory diffusible signal to APC/C^{Cdc20}, whose nature, although not yet completely understood, prevents anaphase onset until all chromosomes are adequately attached and aligned (Bharadwaj and Yu, 2004; Kops *et al.*, 2005; May and Hardwick, 2006).

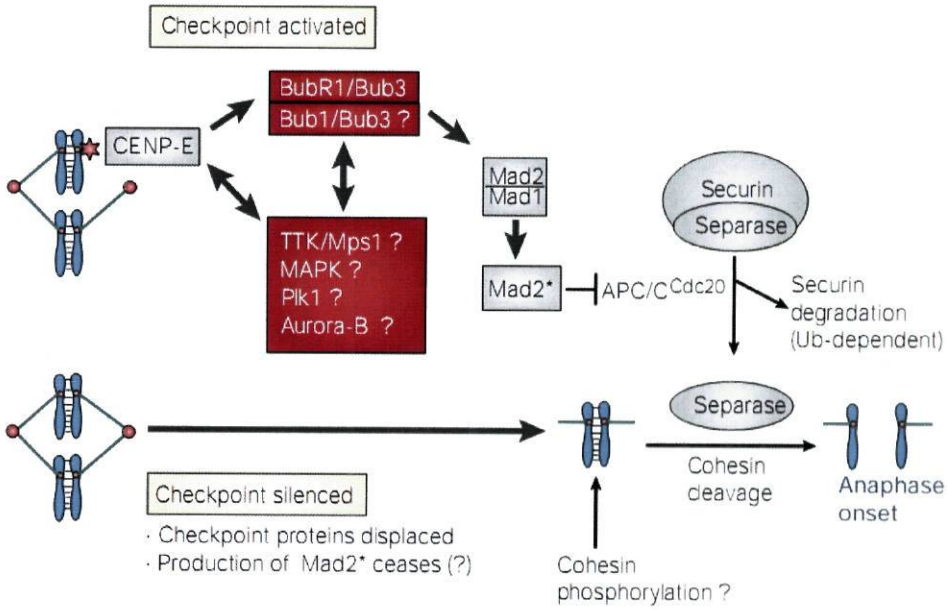

Fig. 1.6: The spindle assembly checkpoint. The kinesin-related protein CENP-E interacts with BubR1 and together they translate structural information about the presence or absence of correctly bound microtubules at the kinetochore. If there are non-attached or mis-attached chromosomes, these events are thought to mediate the recruitment of Mad1-Mad2 complexes. Mad2 is then released in a closed conformation (here represented as Mad2*), strongly inhibiting APC/C^{Cdc20}. Securin degradation (normally dependent on ubiquitination (Ub)) is then prevented, thereby inhibiting the cleavage of cohesin by separase. Sister chomatids remain bound until proper kinetochore-microtubule interactions are established. Proteins that have been also found at the kinetochores and whose participation in checkpoint signalling has been reported are also represented (MAPK, Plk1, Aurora B) (Nigg, 2001).

APC/C inactivation proceeds whenever there are non-attached or mis-attached chromatids, through Cdc20-mediated recruitment of Mad2, Bub3 and BubR1 (Bub1-related protein, the vertebrate homolog for yeast Mad3). Together, these proteins constitute, in near equal stoichiometry (Hoyt, 2001), a quaternary assembly, the mitotic checkpoint complex (MCC), which acts to sequester and inhibit APC/C regulatory protein Cdc20 (Bharadwaj and Yu, 2004; Schmidt and Medema, 2006; Logarinho and Bousbaa, 2008). Currently, it is accepted that kinetochores may act as a catalytic platform for MCC assembly or, alternatively, that they activate checkpoint proteins to form MCC at the cytosol and to sensitize APC/C for inhibition (Logarinho *et al.*, 2008; Musacchio and Salmon, 2008).

Kinetochore-associated CENP-E binds to BubR1, activating its kinase activity, which is, in turn, necessary for the recruitment of a stable Mad1-Mad2 heterodimer (Kops *et al.*, 2005; Logarinho *et al.*, 2008). Indeed, fully inactivation of APC/C is reached by the synergistic interaction between Mad2 and BubR1, which show a lower inhibitory potential when acting independently (May and Hardwick, 2006). Together with other essential

checkpoint proteins, the Mad1-Mad2 heterodimer activates Mad2 which, in conjunction with BubR1 and Bub3, strongly combine with Cdc20 and prevent it from activating the APC/C. MCC-promoted sequestration of Cdc20 compromises APC ubiquitin ligase activity, which is essential for anaphase onset, as explained before (**fig. 1.6**) (Kops *et al.*, 2005; Schmidt and Medema, 2006; Logarinho and Bousbaa, 2008). Thus, in normal situations, only when all the conditions are gathered does the cell progress into anaphase; otherwise, it remains blocked in the metaphase-to-anaphase transition.

Although controversial, the activation of the mitotic checkpoint response is more likely to be the result of a combination of both lack of microtubule attachment and of the consequent lack of physical tension between sister kinetochores (Bharadwaj and Yu, 2004; Pinsky and Biggins, 2005; May and Hardwick, 2006). When all chromosomes undergo bipolar attachments to spindle microtubules, tension between sister kinetochores promotes checkpoint silencing and anaphase onset (Zhou *et al.*, 2002; Schmidt and Medema, 2006). Anaphase inhibitory complexes must then be disassembled and mitotic checkpoint proteins must be withdrawn from the kinetochores. Dynein and dynactin play a crucial role in checkpoint protein transport from the kinetochores to the spindle poles (Howell *et al.*, 2001; Bharadwaj and Yu, 2004). Mad2 stops being recruited to the kinetochores and the MCC is no longer produced; Cdc20 dissociates from Bub1 and Mad2 and binds to the APC, rendering it active (Sudakin *et al.*, 2001; Musacchio and Salmon, 2007). Securin is then degraded, which releases separase for cohesin cleavage. Cells finally enter anaphase, which is also promoted by cyclin B destruction (Peters, 2002; Kops *et al.*, 2005; Logarinho and Bousbaa, 2008).

When cells are not capable of satisfying SAC requisites after a long mitotic delay, they may have different fates: some of them die during mitosis, others exit mitosis but die via apoptosis in G1, and others exit mitosis but are tetraploid and reproductively dead (Niikura *et al.*, 2007).

1.4 Checkpoint defects, aneuploidy and cancer

It has been over than 100 years since Theodor Boveri first hypothesized a causal connection between genome mis-segregation, the disadvantageous effects that it has on cells and their progeny, and the development of tumour cells (Kops *et al.*, 2005; Weaver and Cleveland, 2005). Indeed, genetic instability lies beneath some pathological disorders, being correlated with premature ageing, inherited diseases and predisposition to cancer in humans (Aguilera and Gómez-González, 2008).

Aneuploidy has generally a dramatic impact over cells, in which, under normal conditions, the checkpoint response is chronically activated. Cells enter interphase without cytokinesis, which is normally followed by apoptosis-mediated cell death (Kops *et al.*, 2005; Schmidt and Medema, 2006). However, tumour cells constitute an exception to this observation – most solid tumour cells exhibit chromosome rearrangements and are aneuploid. Different cancer cell lines present 'chromosomal instability' (CIN), which means that they frequently gain or lose whole chromosomes along with their divisions (Bharadwaj and Yu, 2004; Kops *et al.*, 2005; Aguilera and Gómez-González, 2008).

Some tumours are stably aneuploid, which implies that, at some point in their evolution, their cells suffered from a chromosomal redistribution that has somehow conferred them a proliferative advantage. For instance, in a considerable number of colorectal cancer cell lines, CIN was detected (Grabsch *et al.*, 2003; Grabsch *et al.*, 2004; Abal *et al.*, 2007) and chromosome content was shown to undergo constant rearrangements. The exact mechanism that lies behind these chromosomal imbalances is not precisely established, but one of the most accepted theories postulates that their origin resides in the combination of defects in apoptosis-related machinery and the occurrence of failures in the processes that monitor chromosome segregation during mitosis, one of them being the spindle assembly checkpoint (Kops *et al.*, 2005; Schmidt and Medema, 2006).

Furthermore, it is now known that all human aneuploidies (cells that display an abnormal chromosome content and number, i.e., a number other than 46) that occur during development end in embryonic lethality or, in the scarce cases in which they do not, result in serious birth defects. A complete inactivation of certain checkpoint genes in higher organisms (e.g., Mad2 and Bub1) has the same effect, suggesting that spindle checkpoint may be crucial for early development of multicellular organisms or that these genes may have non-checkpoint functions yet to be identified (Bharadwaj and Yu, 2004).

Aneuploidy may result from different phenomena. Aberrant mitotic processes, in addition to deficiencies in centrosome duplication, maturation and segregation, explain episodes of divisions occurring in the presence of multipolar mitotic spindles, which, in turn, generate aneuploid daughter cells. Chromosome cohesion defects may equally justify aneuploidy appearance in some tumours. A third possibility refers to inappropriate attachment of chromosomes to spindle microtubules; for instance, merotelic attachments, in which the same kinetochore is simultaneously connected with microtubules from both poles, are a common cause of aneuploidy. In colorectal tumours, 90% of which exhibit CIN, mutations in *APC* seem to be the main responsible for aneuploidy (Tighe *et al.*, 2001; Kops *et al.*, 2005). On one hand, their proliferation is enhanced due to the inability to degrade β-catenin; on the other hand, because kinetochore-microtubule interactions are

destabilized, chromosomes mis-segregate during anaphase. Lastly, molecular defects that weaken the mitotic checkpoint response induce aneuploidy by propitiating premature chromosome segregation (Kops *et al.*, 2005).

Mutations in the genes encoding for checkpoint proteins themselves have also been identified in some human cancers, although they are rare. For instance, in some colorectal cancer cell lines, cells presented mutations in one of the Bub1 alleles, and some other mutations have been thereafter detected in several studies using CIN cancer cell lines. It is believed that mutations affecting nonidentified spindle checkpoint genes may also account for other tumours where CIN has been reported (Nigg, 2001; Bharadwaj and Yu, 2004; Grabsch, 2004).

Nevertheless, aneuploid tumour cell lines do not necessarily present mutations in the known spindle checkpoint genes. In many of them, the observed checkpoint defects are linked to altered expression levels of spindle checkpoint proteins. Even relatively minor alterations of this nature can catalyse tumorigenesis, as demonstrated by Michel *et al.* (2001) in mice with reduced Mad2 levels that showed a high incidence of lung tumours (Bharadwaj and Yu, 2004). Moreover, Mad2 promoter silencing has been implicated in human hepatocellular carcinogenesis; also, reduced Mad2 expression levels, as well as Bub1 overexpression, have been positively correlated with a deregulated SAC function and CIN in a breast cancer cell line (Yuan *et al.*, 2006). Overexpression of Bub1, Bub3 or BubR1 is frequent among human gastric cancers, in which Mps1 upregulation has also been documented (Rimkus *et al.*, 2006; Schmidt and Medema, 2006).

The association of the CIN phenotype with mutations in spindle checkpoint genes, decreased levels of spindle checkpoint proteins and loss or diminishment of the spindle checkpoint response strongly suggest a close relation between altered activity of the mitotic checkpoint and tumorigenesis (Niikura *et al.*, 2007).

Since even tumour cells tolerate CIN only to a limited degree (as pronounced deviations from the normal karyotype might seriously compromise cell viability), it is more likely that partial disruption of the spindle checkpoint is more commonly observed in these cells than complete inactivation of the checkpoint response (Bharadwaj and Yu, 2004). Anyway, it is certain that cell viability-compatible karyotypic abnormalities correlate with poor prognosis in most cases (Nigg, 2001).

1.5 Medulloblastoma and Malignant Peripheral Nerve Sheath Tumour

Brain tumours are the most common solid tumours during infancy and the second main form of cancer after leukaemias, constituting also the major cause of oncologic mortality in paediatrics. Additionally, combined effects of the pathology and of its treatment represent main morbidity causes (Yazigi-Rivard *et al.*, 2008).

Medulloblastoma is a highly malignant cerebellar tumour, the most prevalent malignant brain tumour in childhood. It originates in the cerebellum or posterior fossa, possibly from cerebellar granule cell precursors (CGNPs) (Uziel *et al.*, 2006; Yazigi-Rivard *et al.*, 2008), and is included in the family of cranial primitive neuroectodermal tumours (PNET). Tumours arise with a similar prevalence in the cerebellar vermis (mainly in children) and in the cerebellar hemispheres (in older patients), and often invade the fourth ventricle, with occasional brainstem involvement (Collins, 2004; Yazigi-Rivard *et al.*, 2008). Evidence suggests that medulloblastomas may result from CGNPs that accumulate oncogenic mutations and are not eliminated by cell cycle control mechanisms that, in turn, depend primarily upon the retinoblastoma protein (Rb) and p53, thereby failing to correctly exit the cell cycle and differentiating. This way, medulloblastoma cell precursors are provided (Uziel *et al.*, 2006).

It occurs mostly in children aged 5 to 10 years and accounts for 20-30% of all paediatric brain tumours (Wechsler-Reya, 2003; von Bueren *et al.*, 2007; Yazigi-Rivard *et al.*, 2008), representing 14.5% of newly diagnosed cases (Gurney *et al.*, 2000). In adults, the disease is rather rare, corresponding to less than 2% of all central nervous system malignancies (Wechsler-Reya, 2003; von Bueren *et al.*, 2007; Yazigi-Rivard *et al.*, 2008). Medulloblastoma has a higher incidence in males (62%) than in females (38%). Furthermore, it is more common in younger children than in older children; 40% of all cases are diagnosed before the age of 5, 31% are between the ages of 5, 18.3% between the ages of 10 and 14, and 12.7% between the ages of 15 and 19 (von Bueren *et al.*, 2007).

Several lines of evidence suggest that defects in the Sonic hedgehog-Patched signalling pathway, present in ~30% of cases, are implied in the pathogenesis of medulloblastoma (Wechsler-Reya, 2003; Ferretti *et al.*, 2005; Uziel *et al.*, 2006; Yazigi-Rivard *et al.*, 2008). Sonic hedgehog (Shh), a molecule secreted by the cerebellar Purkinje neurons, functions as a master regulator of embryonic development and of proliferation in the developing cerebellum. Patched (Ptch), in turn, is a transmembrane protein that acts as both a Shh receptor and an antagonist of its signalling. In effect,

mutations in the human Ptch gene have been identified in patients with Gorlin's syndrome, a disease with increased incidence of medulloblastoma. Many sporadic medulloblastomas, especially those of the desmoplastic subtype, have also been associated with mutations in Ptch and other components of the Shh-Ptch pathway (Wechsler-Reya, 2003; Collins, 2004; Pogoriler, 2006).

Mutated elements of the Wnt signalling pathway have been related to medulloblastoma development as well (Wechsler-Reya, 2003; Uziel *et al.*, 2006). For instance, Turcot's syndrome, which derives from mutations in the APC gene, is characterized by a high incidence of colorectal cancers and brain tumours, namely medulloblastoma (Wechsler-Reya, 2003; Collins, 2004; Pogoriler, 2006). In fact, APC mutations were reported in about 4% of sporadic medulloblastomas, of which 8-15% have been shown to harbour activating mutations in β-catenin and 12% in axin, a negative regulator of Wnt signalling. Thus, a subset of medulloblastomas may derive from activation of the Wnt pathway (Wechsler-Reya, 2003). Mutations affecting the NOTCH signal transduction pathway have also been described in medulloblastomas, though genetic lesions behind the majority of these tumours still remain unidentified (Uziel *et al.*, 2006).

Several other studies using medulloblastoma cells have proven their overexpression of transcription factors N-myc, c-myc (Li *et al.*, 2005; von Bueren *et al.*, 2007), pax5 and zic and of the receptor tyrosine kinase ErbB2 (Wechsler-Reya, 2003; Collins, 2004). It remains uncertain whether these genes participate in the development and/or progression of medulloblastomas or if they simply constitute molecular markers of the transformed cell type (Wechsler-Reya, 2003). The PDGF receptors and ligands are also being investigated for their eventual significance in medulloblastoma biology (Collins, 2004).

Cytogenetic techniques have revealed that 30 to 50% of human medulloblastomas carry a deletion or rearrangement of part of chromosome 17 (Wechsler-Reya, 2003; De Smaele *et al.*, 2004; Ferretti *et al.*, 2005). In most cases, isochromosome 17q [i(17q)] is the observed karyotypic abnormality. Most of the short arm (17p) is lost from two chromosomes 17 and they fuse head-to-head, producing a chromosome with two centromeres, little 17p and two long arms (17q) (Wechsler-Reya, 2003; Collins, 2004; Ferretti *et al.*, 2005). This genetic lesion may account for Shh pathway deregulation in the cases where no mutations in its components are detected (Ferretti *et al.*, 2005). The fact that this rearrangement is frequently also identified in leukaemias, lymphomas and stomach, colon and cervix cancers suggests that at least one potent tumour suppressor is located on chromosome 17p short arm (Wechsler-Reya, 2003). This putative tumour suppressor is believed to localise to 17p13.3, a region containing about 20 known genes,

including those encoding the lissencephaly-associated protein Lis1, the breakpoint cluster region-related gene *ABR*, the Max-binding protein Mnt, and the transcription factor hypermethylated in cancer-1 Hic1, although none of them have been conclusively linked to medulloblastoma etiology (Wechsler-Reya, 2003). In this context, it has been asserted that chromosome 17p deletion leads to the loss of REN(KCTD11), a novel Hedgehog antagonist, thus abolishing a checkpoint of Shh-dependent events during cerebellum development and tumorigenesis (De Smaele *et al.*, 2004; Ferretti *et al.*, 2005). Similarly, p53 tumour suppressor also maps to 17p13 region; its inactivation cooperates with Shh pathway for medulloblastoma formation, providing haploinsufficiency conditions that cause abrogation of direct and indirect checkpoints of Shh signalling in cancer (De Smaele *et al.*, 2004). 10q loss is one of the many other chromosomal aberrations that have been correlated with medulloblastoma (Collins, 2004).

Malignant peripheral nerve sheath tumour (MPNST) is a rare variant of soft tissue sarcoma of ectomesenchymal nature. World Health Organization has devised the term MPNST, allowing the replacement of previous heterogeneous and frequently confusing terminology, such as malignant schwannoma, malignant neurilemmoma, and neurofibrosarcoma, for tumours of neurogenic origin and similar biological behaviour (Kar *et al.*, 2006). MPNST diagnosis is often made difficult due to the similarities with other spindle cell sarcomas. The tumour arises from a major or minor peripheral nerve branch or sheath of peripheral nerve fibres. It may be of spontaneous origin in adult patients, even if 5 to 42% of MPNST cases are associated with multiple neurofibromatosis Type-I (Kobayashi *et al.*, 2006). Multifocality and development of second primary tumours presenting the same histology are other clinical features of the disease. Surgery is the preferred treatment for this aggressive tumour (Kar *et al.*, 2006).

Many structural and numerical chromosomal aberrations have been described in MPNST (Kobayashi *et al.*, 2006). p53 mutations were proven to contribute to the development of the disease (Berghmans *et al.*, 2005).

1.6 Aim of the study

Medulloblastoma is the most common primary central nervous system tumour that arises in childhood, comprising 20-30% of all paediatric brain tumours. Like in many other neoplasms, medulloblastoma cells are genetically unstable, reflecting chromosome gain or loss when cell division takes place. The molecular basis behind medulloblastoma aneuploidy is not completely known. Nonetheless, structural and numerical karyotypic abnormalities, as well as mutations in key components of pathways involved in development and cell proliferation, have been reported in medulloblastoma cells, which leads to the suspicion that mitotic checkpoint anomalies may contribute to the neoplasm's pathogenesis and/or malignancy.

In view of medulloblastoma's high representativeness among paediatric tumours and of the scarcity of studies concerning mitotic checkpoint activity in cells from this pathology, the present work aims at evaluating the mitotic checkpoint competence in medulloblastoma cells and identifying the molecular alterations that lie beneath eventual defects in its activity.

In effect, the amount of works done in this field is far from being satisfactory and from clarifying the eventual participation of mitotic checkpoint defects in the development of medulloblastoma tumour cells. Taking that into consideration, the present study aims at complementing the currently available knowledge concerning medulloblastoma pathogenesis, namely by characterizing mitotic checkpoint efficiency. Eventual mitotic checkpoint abnormalities, as well as the underlying molecular alterations, are investigated, using the Daoy medulloblastoma-derived cell line.

2. Materials and Methods

2.1 Cell lines

Three different human tumour cell lines were used: HeLa – cervical cancer – (Molecular Medicine Institute, University of Lisbon, Portugal), S462 – Malignant Peripheral Nerve Sheath Tumour – and Daoy – medulloblastoma – (ICVS, University of Minho, Braga, Portugal).

Although they derive from neoplastic tissue, the efficacy of the mitotic checkpoint in HeLa cells is well documented, and they constituted the experimental control in all the experiments.

2.1.1 Cell culture conditions

HeLa, S462 e Daoy cells were cultured in complete growth medium consisting of Dulbecco's Modified Eagle Medium (D-MEM) supplemented with 10% (v/v) Foetal Bovine Serum (FBS), 1% (v/v) GlutaMAX and 1% (v/v) Antibiotic-Antimycotic mixture (10,000 units/ml penicillin G sodium, 10,000 µg/ml streptomycin sulfate and 25 µg/ml amphotericin B as Fungizone®, in 0.85% saline). Unless otherwise stated, all reagents were purchased from Invitrogen. Cells were cultured in a monolayer, in tissue culture flasks (Orange Scientific) and kept in exponential growth in a humidified incubator (Heraeus Hera cell) at 37.0 °C and a 5.0% CO_2 atmosphere. All cell culture-related proceedings were done in a Nuaire™ laminar flux biological safety cabinet, biosafety level II, type A/B3.

2.1.2 Cell subculture

Cells were splitted before reaching total confluence, in order to avoid suffering from space and nutrient depletion. Growth medium was aspirated and the cells were washed with 2 ml of sterile Phosphate-Buffered Saline (PBS, pH 7.2: 137 mM NaCl; 2.7 mM KCl; 6.4 mM K_2HPO_4; 1 mM $NaHPO_4$) and incubated with 1 ml of 0.25% Trypsin EDTA 1×. After a 2 to 3 minute-incubation at 37.0 °C, cell detachment was confirmed by microscopic observation. 1 volume of complete growth medium was added to stop the reaction and a 30 µl aliquot of cell suspension was collected. 30 µl of trypan blue were then added to this aliquot. After a 5 minute-incubation, an aliquot of 10 µl was transferred to a Neubauer counting chamber. Cells were then counted using the trypan blue exclusion

method and cell density (number of cells per ml) was determined[1]. Finally, a volume equivalent to 0.2 x 10^6 cells or to 0.4 x10^6 cells (unless otherwise stated) was transferred to a final volume of 5 or 13 ml of fresh growth medium, respectively.

2.1.3 Cell line thawing

Cell lines were stored in Recovery™ – Cell Culture Freezing Medium, containing 10% (v/v) DMSO, in liquid nitrogen. A cryovial containing cells was removed, rapidly thawed in a 37 °C water bath, and the cells were transferred to pre-warmed growth medium. This medium was replaced 6 hours later (or, alternatively, the following day) due to DMSO toxicity, then periodically during culture.

2.1.4 Cell line freezing

Cells were stored when growing exponentially in order to maintain a stock for posterior thawing and preventing phenotypic degeneration. Cell suspensions were obtained as mentioned in **section 2.1.2** and centrifuged at 1,000 rpm for 5 minutes; the supernatant was discarded. Each pellet (1.0 to 2.0 x 10^6 cells) was then gently resuspended in 1 ml Recovery™ – Cell Culture Freezing Medium containing 10% (v/v) DMSO, and transferred to adequate cryovials. Upon remaining 15 minutes at room temperature, the cryovials were transferred to -80 °C for 24-48 hours and finally stored in liquid nitrogen.

2.2 Cell synchronization

0.08 x 10^6 cells from each cell line were seeded onto 35 mm individual Petri dishes (Orange Scientific) and maintained under the conditions that ensure their optimal growth. When they became about 70% confluent, thymidine (Sigma-Aldrich) was added to growth media at a final concentration of 2 mM. After 18 to 19 hours of incubation, it was verified, by phase contrast microscopy in a Nikon Eclipse TE2000-U microscope, that cells were successfully synchronized in G1/S transition, due to the absence of mitosis. Cells were then released by removing the culture media, washing three times with PBS and incubating with thymidine-free growth medium. 11 to 12 hours later, phase contrast observations confirmed that cells had achieved mitosis.

[1] $$\text{No. of cells/ml} = \frac{\text{total cell number}}{\text{number of squares}} \times \text{dilution factor} \times 10^4$$

2.3 Mitotic index determination

Cells from each cell line were synchronized as detailed in **section 2.2**. Nocodazole (Sigma) was added to a final concentration of 0.5 μM three hours after the release. Mitotic index (MI) was determined by cell-rounding under phase contrast microscopy (Nikon Eclipse TE2000-U microscope), as the percentage of mitotic cells in relation to total cell number (mitotic and interphase cells). Determinations were done upon 0, 9, 15, 21, 27 and 48 hours after the release. Controls were submitted to the same treatment, but with no nocodazole addition. Three independent determinations were done for each experimental situation, and a mean value was then calculated.

2.4 Immunofluorescence

For immunofluorescence, cells were seeded in 35 mm Petri dishes (Orange Scientific) onto 22-mm poly-L-lysine pre-treated glass coverslips two days prior to the experiment. They were removed from growth medium and fixed either immediately or after a 3 hour-incubation with 0.5 μM nocodazole (**protocol 2**). According to the proteins/structures to detect by fluorescence microscopy in each experience, two variants of the immunofluorescence protocol were used. For the vast majority of the purposes, **protocol 1** was used, while **protocol 2** was followed when preservation of microtubules was relevant.

Protocol 1. Cells were fixed in freshly prepared 2% (w/v) paraformaldehyde (PFA, Sigma) in 1× PBS for 7 minutes at room temperature. They were then washed three times for 5 minutes with 1× PBS. Upon washing, cells were permeabilized by incubating for 7 minutes with 1× PBS containing 0,2% (v/v) Triton X-100. Following permeabilization, cells were washed three times for 5 minutes with PBST (1× PBS containing 0.05% (v/v) Tween-20). In order to prevent non-specific binding, cells fixed onto the glass coverslips were incubated with blocking buffer (PBST containing 10% (v/v) FBS). They were then labelled with primary antibodies, diluted in PBST containing 5% (v/v) FBS. Different primary antibodies were employed: rabbit anti-Bub1 (1:3000, Abcam), mouse anti-BubR1 (1:600, Chemicon International), mouse anti-Bub1 and sheep anti-BubR1 (1:2000, gifts from S. Taylor, School of Biological Sciences, University of Manchester), human anti-CREST (1:1500, courtesy of E. Bronze-da-Rocha, IBMC, Porto) and mouse or rabbit anti-α-tubulin (1:2000, Sigma and Abcam, respectively). Cells were then washed three times for 5 minutes with PBST. Secondary antibodies were diluted 1:1500 in PBST containing 5% (v/v) FBS. Alexa Fluor® 488- and 568-conjugated secondary antibodies (Molecular

Probes, Invitrogen Detection Technologies) were used in accordance with primary antibodies' sources. Incubations with blocking buffer, primary and secondary antibodies proceeded within a humidified chamber, for 1 hour at room temperature. Cells were washed again with PBST three times for 5 minutes and, finally, they were washed once with 1× PBS for 5 minutes. Each coverslip was mounted in 8 µl Vectashield containing 0.5 µg/ml DAPI and secured with nail polish.

Protocol 2. Cell fixation was done by incubating with methanol for 2 minutes at -20 °C. Cells were then carefully washed with Tris-Buffered Saline (TBS: 20 mM Tris HCl, pH 7.4; 150 mM NaCl). Permeabilization consisted of a 5 minute-incubation with TBS containing 0.5% (v/v) Triton X-100, at room temperature, followed by three 1.5 minute-washings with TBS containing 0.05% (v/v) Triton X-100. Blocking and antibody dilutions were done as in **protocol 1**, except that TBS was used in place of PBS. Immunofluorescence images were acquired using a 60× apochromatic objective, on a Nikon Eclipse TE2000-U microscope equipped with a DXM1200F digital camera and controlled by Nikon ACT-1 software. Representative focus plans were chosen for image acquisition.

2.5 Chromosome spread

Chromosome spread experiments were performed after 0, 12 and 24 hours of exposure to nocodazole. Mitotic cells were shaken off and collected into a Falcon tube (Orange Scientific). In order to promote hypotonic shock, bidistilled water (pre-warmed in a 37 °C water bath) was added to each cell suspension (60% of the volume of the cell suspension). The mixture was gently homogenized and incubated for 5 minutes at 37 °C. It was then centrifuged at 1,000 rpm for 5 minutes. The supernatant was discarded with the aid of a pipette and the pellet was resuspended in 2 ml of a 75% (v/v) methanol:25% (v/v) acetic acid solution. Cell fixation in this mixture proceeded for 2 minutes at room temperature. The suspension was again centrifuged and fixed according to the abovementioned. The supernatant was discarded again, leaving just 100 to 200 µl of it for resuspending the pellet with a micropipette. This final suspension was transferred to a microscope glass slide, dried overnight and was finally mounted in 8 µl Vectashield containing 0.5 µg/ml DAPI.

2.6 Preparation of protein extracts

Growth media in the culture flasks were recovered, cells were washed with PBS and their detachment was promoted by incubating with Trypsin EDTA for 3 minutes. The reaction was stopped by adding one volume of growth medium and the resulting suspensions were combined with the growth media initially collected. The mixtures were then centrifuged at 1,000 rpm for 5 minutes and the supernatants were discarded. Each pellet was resuspended in 160 µl RIPA lysis buffer 1× (Santa Cruz Biotechnology), which was previously supplemented with PMSF, protease inhibitor cocktail and sodium orthovanadate solutions (also supplied in the product) according to manufacturer directions. The solution was collected into an ice-cold Eppendorf microcentrifuge tube. In order to promote cell lysis, the solution was sheared through a syringe-adapted needle. The lysate was allowed to sit for 20 minutes on ice and was then centrifuged at 13,000 rpm, for 5 minutes and at 4 °C using a Heraeus Biofuge primo R refrigerated centrifuge.

150 µl of the supernatant were reserved for Western blotting and 10 µl for protein quantification. Additional 30 µl of 6× SDS-PAGE sample buffer (0.35 M Tris HCl, pH 6,8; 30% (v/v) glycerol; 10% (w/v) SDS; 9.3% (w/v) DTT; 0.25% (w/v) bromophenol blue) were added to each 150 µl Western blotting sample portion. Then, the tubes were placed on a heating block and protein samples were boiled at 100 °C for 3 minutes, and then back onto ice. All samples were frozen at -80 °C.

2.6.1 Protein quantification

Protein quantification assays were performed by Optical Density (OD) spectrophotometry measurements at 562 nm, using the BCA™ Protein Assay Kit (Pierce Biotechnology), by mixing 50 parts of Reagent A with 1 part of Reagent B and following the standard test tube procedure protocol. Protein samples were thawed and diluted ten-fold in distilled water before colour development.

2.7 Western blotting

2.7.1 Protein separation by SDS-PAGE

Protein samples were analyzed by Western blot, by first separating protein bands by SDS-PAGE. The gel was formed with 10% polyacrylamide resolving gel (for all the proteins except for Bub3, which was resolved through a 15% gel) and 6% polyacrylamide stacking gel. A Mini-PROTEAN® 3 system (Bio-Rad Laboratories) was used for

electrophoresis assays. It was filled with running buffer (25 mM Tris HCl, pH 8.3; 192 mM glycine; 0.1% (w/v) SDS); then, a volume of sample equivalent to 15 µg of protein (except for Bub3 blots, in which 20 µg were used) were loaded into the appropriate wells. The apparatus was run at constant voltage (200 V/gel), for 60 minutes, until the dye front reached the bottom of the polyacrylamide gel.

2.7.2 Membrane transfer

At the end of electrophoresis, the gels were equilibrated in transfer buffer (192 mM glycine; 25 mM Tris base; 20% (v/v) methanol, pH 8.3), as well as blotting papers (Quickdraw™, Sigma-Aldrich) and nitrocellulose transfer membranes (Hybond™-ECL™, Amersham Biosciences). Gel transfer was done at 110 mA per gel for 75 minutes, using a Hoefer SemiPhor Transphor Unit (semi-dry transfer unit) from Amersham Pharmacia Biotech. Voltage was carefully monitored to ensure it did not surpass 25 volts. The efficiency of the transfer process was assessed by membrane staining with Ponceau S (0.5% (w/v) Ponceau S; 5% (w/v) trichloroacetic acid).

2.7.3 Blotting

The transferred membranes were washed in Tris-Buffered Saline and Tween-20 (TBST: 137 mM NaCl; 20 mM Tris base; 0.1% (v/v) Tween-20) to remove any remaining acrylamide. Non-specific sites were blocked with appropriate blocking buffer (5% (w/v) non-fat dry milk in TBST). The membranes were then washed with a solution of 1% (w/v) non-fat dry milk in TBST, for 10 minutes at room temperature. Various primary antibodies were used: mouse anti-Bub1 and sheep anti-BubR1 (1:2000, courtesy of S. Taylor, School of Biological Sciences, University of Manchester), mouse anti-Bub3 (1:1000, BD Transduction Laboratories) and mouse or rabbit anti-α-tubulin (1:2000, Sigma or Abcam, respectively). α-Tubulin blots were used as loading controls. Incubations with blocking buffer, primary and secondary antibodies proceeded for 1 hour each, at room temperature and with constant agitation. Primary and secondary antibodies were diluted in a solution of 1% (w/v) non-fat dry milk in TBST.

2.7.4 Developing Westerns

After incubation with primary antibody solution, blots were washed in a solution of 1% (w/v) non-fat dry milk in TBST for 10 minutes. They were then incubated with the appropriate horseradish peroxidase (HRP)-conjugated secondary antibody solutions. Peroxidase labelled anti-rabbit IgG, anti-mouse IgG (Sigma) and anti-sheep IgG (Abcam)

were diluted 1:3000 and employed according to primary antibodies' sources. Membranes were then washed twice with TBST for 10 minutes and, finally, once with TBS.

For development, the Enhanced Chemiluminescence (ECL) method was performed; equal parts of Western Lighting Chemiluminescent Reagent Plus oxidizing solution and enhanced luminol reagent (ECL solutions A and B, respectively) were mixed after the third wash. Each blot was then immersed in the resulting ECL solution (0.198 mM coumaric acid; 1.25 mM luminol; 0.009% (v/v) H_2O_2; 100 mM Tris HCl, pH 8.5) for 3 minutes before being sealed between plastic for development.

Blots were placed in a photo cartridge (Hypercassette™, Amersham Biosciences) and exposed to Kodak BioMax Light Film (Sigma-Aldrich) in the darkroom, for varying amounts of time, before development. Autoradiographic films were automatically developed.

2.7.5 Densitometry

For the quantitative analysis of protein expression, films obtained through the ECL detection system were scanned in a Gel Doc™ XR densitometer and band intensities were quantified using The Discovery Series™ Quantity One® 1-D analysis software, version 4.6.1, both from Bio-Rad Laboratories, Inc.

2.8 Real-Time PCR (two-step procedure)

2.8.1 RNA isolation and analysis

All RNA-related manipulation precautions were taken during its isolation. Water and all necessary glassware and autoclavable items were DEPC-treated, while work surfaces and pipettes were periodically wiped with a 0.5 M NaOH solution and nonautoclavable plasticware was occasionally rinsed with a 0.1 M NaOH, 1 mM EDTA solution.

0.8×10^6 cells from each cell line were seeded onto 10 cm^2 Petri dish plates (Nunclon™ Δ Surface, Nunc) and maintained under optimal growth conditions. When they reached about 70% confluence, total RNA extracts from HeLa, S462 and Daoy cell lines were prepared employing PureZOL™ RNA Isolation Reagent (Bio-Rad Laboratories) and following supplier's instructions concerning cells growing in a monolayer. Growth medium was aspirated and 1 ml PureZOL™ RNA Isolation Reagent was added to each dish plate. Up and down pipettings were done in order to promote cell lysis. A 5 minute-incubation at

room temperature allowed the complete dissociation of nucleoprotein complexes. Lysates were collected and 200 µl chloroform were added to each of them. These mixtures were vigorously shaken for 15 seconds and were then incubated for 5 minutes at room temperature, with periodical mixings. They were centrifuged at 12,000 *g* for 15 minutes and at 4 °C. Upon centrifugation, the (upper) aqueous phases were collected into new RNase-free tubes, to which 500 µl isopropyl alcohol were added. After thoroughly mixing and a 5 minute-incubation at room temperature, the mixtures were again centrifuged at 12,000 *g* for 10 minutes and at 4 °C. Supernatants were carefully discarded and the resulting pellets were washed with 1 ml 75% (v/v) ethanol, vortexed and finally centrifuged at 7,500 *g* for 5 minutes and at 4 °C. Supernatants were discarded and pellets were allowed to air-dry for about 5 minutes, upon which they were resuspended in 50 µl of RNase-free water, divided into 10 µl aliquots and stored at -80 °C. In quantitative Real-Time PCR experiments, a total RNA sample from a normal astrocyte cell line, kindly provided by Rui Reis (ICVS, University of Minho, Portugal), was also included. RNA quantification was performed by OD measurements at 260 nm. RNase-free deionised water was used as blank, as well as solvent for sample dilutions. 1 OD unit (260 nm) was considered to be equivalent to 50 µg/ml RNA. RNA quality was evaluated by electrophoretic analysis of sample volumes equivalent to 1 µg RNA in 0.8% (w/v) RNase-free agarose gels, as well as by the $OD_{260\ nm}$ / $OD_{280\ nm}$ ratio.

2.8.2 Quantitative Real-Time Polymerase Chain Reaction

- ***Primer design***

Forward and reverse primers were designed using Beacon Designer 7.2 (Bio-Rad Laboratories) and PerlPrimer version 1.1.14 (http://perlprimer.sourceforge.net) softwares (**table 2.1**) and were obtained from STABvida (Oeiras, Portugal). For subsequent applications, they were reconstituted in water to a final concentration of 10 µM.

Gene	Primer	Pairing Position in the cDNA	Length of the Amplified Sequence (bp)	Primer Oligonucleotide Sequence
GAPDH	Forward	49	101	5'-ACA GTC AGC CGC ATC TTC-3'
	Reverse	149		5'-GCC CAA TAC GAC CAA ATC C-3'
Cdc20	Forward	421	151	5'-CCA GAG GGT TAT CAG AAC AG-3'
	Reverse	571		5'-CCA CAA GGT TCA GGT AAT AGT-3'
Bub1	Forward	463	171	5'-CAA GCT AGA ACC TCA GAA CC-3'
	Reverse	633		5'-CAC TCT TCG TTC CAT ATT TGA C-3'
BubR1	Forward	512	82	5'-CAG ATG CGA TAT TTC AGG AAG GG-3'
	Reverse	593		5'-GCT TGG AAT TGT CGG TGC TG-3'
Bub3	Forward	475	117	5'-GTG TTG GTG TGG GAC TTA CG-3'
	Reverse	591		5'-GCT TAA TAC ATA ACC CTG CTT G-3'
Mad2	Forward	205	117	5'-GTG GAA CAA CTG AAA GAT TGG T-3'
	Reverse	321		5'-GTC ACA CTC AAT ATC AAA CTG C-3'
Chfr	Forward	1671	105	5'-AGACATCCTGAAGAATTACCT-3'
	Reverse	1775		5'-TAATCAGACAGCAGAAACACTC-3'

Table 2.1: Sequences of forward and reverse primers used in Real-Time PCR amplification of GAPDH, Cdc20, Bub1, BubR1, Bub3, Mad2 and Chfr genes using cDNA samples from HeLa, astrocyte, S462 and Daoy cell lines.

Prior to their use in Real-Time PCR experiments, a Reverse Transcriptase PCR with isolated HeLa RNA samples was done to confirm absence of genomic DNA amplification for each primer pair. Then, another PCR was run in order to ascertain primer specificity and annealing temperatures. SuperScript™ III One-Step RT-PCR with Platinum® *Taq* DNA Polymerase kit (Invitrogen) was used and reaction mixtures contained 2 µl total HeLa RNA, 25 µl 2× Reaction Mix, 2 µl forward primer, 2 µl reverse primer, 2 µl SuperScript™ RT/Platinum® *Taq* mix and 17 µl autoclaved distilled water. The amplification program, run in a MJ Mini™ Thermal Cycler (Bio-Rad Laboratories), comprised the following steps: 50.0 °C for 20 minutes; 94.0 °C for 1.5 minutes; 94.0 °C for

15 seconds; 60.0 °C for 30 seconds; 72.0 °C for 1 minute. Amplification products were finally run in a 1% (w/v) agarose gel.

- ***cDNA synthesis***

cDNA synthesis was achieved through a reverse transcriptase-mediated reaction, using the iScript™ cDNA Synthesis Kit (Bio-Rad). 1 µg total RNA from each cell line was used as template. Each reaction was composed of 4 µl 5× iScript Reaction Mix, 1 µl iScript Reverse Transcriptase, a volume of RNA template equivalent to 1 µg RNA and nuclease-free water to a final volume of 20 µl. The program consisted of the steps that follow: 25.0 °C for 5 minutes; 42.0 °C for 30 minutes; 85.0 °C for 5 minutes. It was run in a MJ Mini™ Thermal Cycler (Bio-Rad Laboratories). Resulting cDNA samples were stored at -20 °C.

- ***Real-Time PCR assays***

Each cDNA sample was serially diluted 1:1, 1:10, 1:100 and 1:1000 in RNase-free water for standard curve plotting. For each Real-Time PCR run, a master mix was prepared using iQ™ SYBR® Green Supermix kit (Bio-Rad), following its recommendations and containing 100 nM of each primer, 1× iQ SYBR Green Supermix, and 1 µg cDNA in a final volume of 25 µl. RNA template controls, as well as non-template controls (in which sterile deionised water was used in place of template cDNA) were used to confirm absence of genomic DNA and cDNA contamination, respectively. Experiments were done in triplicate for each data point. The thermal cycling conditions comprised an initial denaturation step at 95.0 °C for 3 minutes, 35 cycles at 94.0 °C for 20 seconds, 60.0 °C for 30 seconds and 72.0 °C for 30 seconds. Finally, the melt curve comprised temperatures from 65.0 to 95.0 °C, with increments of 0.5 °C, for 5 seconds. The program was run in a C1000™ Thermal Cycler, interfaced to a CFX96™ Real-Time PCR Detection System, both from Bio-Rad Laboratories. In the end of each program, data were acquired and analysed using CFX Manager™ Software, version 1.0 (Bio-Rad Laboratories). Glyceraldehyde 3-phosphate dehydrogenase (GAPDH) housekeeping gene amplification was used as a control for normalization of gene expression levels. ΔC_T (ΔC_T = Gene C_T – GAPDH C_T) was determined. Differences in expression levels between HeLa, astrocyte and Daoy and S462 cell lines were calculated using $\Delta(\Delta C_T)$ [$\Delta(\Delta C_T)$ = HeLa, S462 or Daoy ΔC_T – astrocyte ΔC_T]. Melting curve analysis was done in order to verify primer specificity. Real-Time PCR products were finally run in 1% (w/v) agarose gels in order to verify band intensities and the existence of single amplification products.

2.9 Statistical analysis

Data were statistically analysed by means of the t-Student's test. p-values<0.05 were considered statistically significant at the 90% confidence level, and p-values<0.01 at the 99% confidence level.

3. Results and Discussion

The spindle assembly checkpoint or mitotic checkpoint is a surveillance mechanism that acts at the metaphase-to-anaphase transition by monitoring kinetochore-to-microtubule attachments. It delays anaphase onset if kinetochore-to-microtubule attachments are absent or incorrect, thus ensuring appropriate chromosome segregation and the fidelity of genetic transmission (Rieder *et al.*, 1994; May and Hardwick, 2006; Logarinho and Bousbaa, 2008).

Medulloblastoma is a highly frequent central nervous system neoplasm in childhood, representing ~20% of all paediatric brain tumours and affecting mostly children under 5 years old (Wechsler-Reya, 2003; von Bueren *et al.*, 2007; Yazigi-Rivard *et al.*, 2008). Medulloblastoma cells present characteristic structural and numerical chromosome aberrations, as well as mutations in important elements of the Shh-Ptch and Wnt pathways, implied in development and cell proliferation (Wechsler-Reya, 2003; Ferretti *et al.*, 2005; Uziel *et al.*, 2006; Yazigi-Rivard *et al.*, 2008). Chromosomal instability, as a result of abnormal chromosome segregation, may derive from a defective mitotic checkpoint activity, which is investigated in this work.

The present study aims at analysing: **(i)** the competence of the mitotic checkpoint, and **(ii)** the molecular alterations underlying the eventually defective checkpoint in the medulloblastoma cell line Daoy.

3.1 The mitotic checkpoint is defective in Daoy cell lines

In order to evaluate Daoy cells' ability to arrest in mitosis when exposed to mitotic stress-inducing conditions, and thus the efficacy of their mitotic checkpoint, cells were synchronized, released and then exposed to nocodazole, a microtubule-disrupting drug. Cell phenotypes were analysed and the mitotic index (the percentage of mitotic cells relative to the total number of viable cells in culture) was determined after different periods of incubation with nocodazole. In the same context, chromosome spread assays were performed so as to ascertain whether sister chromatids in Daoy cells remain bound when exposed to nocodazole, as expected in case of having a functional and efficient mitotic checkpoint.

In a first approach, the cells' response to the incubation with microtubule poisons was evaluated. In order to make certain that nocodazole could be used as a cell cycle disruptor in subsequent experiments, synchronized Daoy, S462 and HeLa cells were incubated for three hours with 0.5 μM nocodazole. Nocodazole is an anti-mitotic agent that disrupts microtubules by binding to β-tubulin and preventing formation of one of the two interchain disulfide linkages, thus inhibiting microtubule dynamics, disrupting the mitotic spindle function, and fragmenting the Golgi complex. Because it interferes with microtubule polymerisation, it impedes mitotic spindle assembly and, therefore, there is no attachment between kinetochores and microtubules. This lack of attachment induces chronic mitotic checkpoint activation and the cell cycle is arrested at G2/M phase. Prolonged contact with nocodazole induces apoptosis in several normal and tumour cell lines. Nevertheless, some cells may metabolically reject the drug, an hypothesis that must then be tested.

Upon exposure to nocodazole, cells were immunostained for microtubule structure visualization. For that, they were stained with an anti-α-tubulin antibody, for the assessment of the effect of nocodazole on microtubules **(fig. 3.1)**.

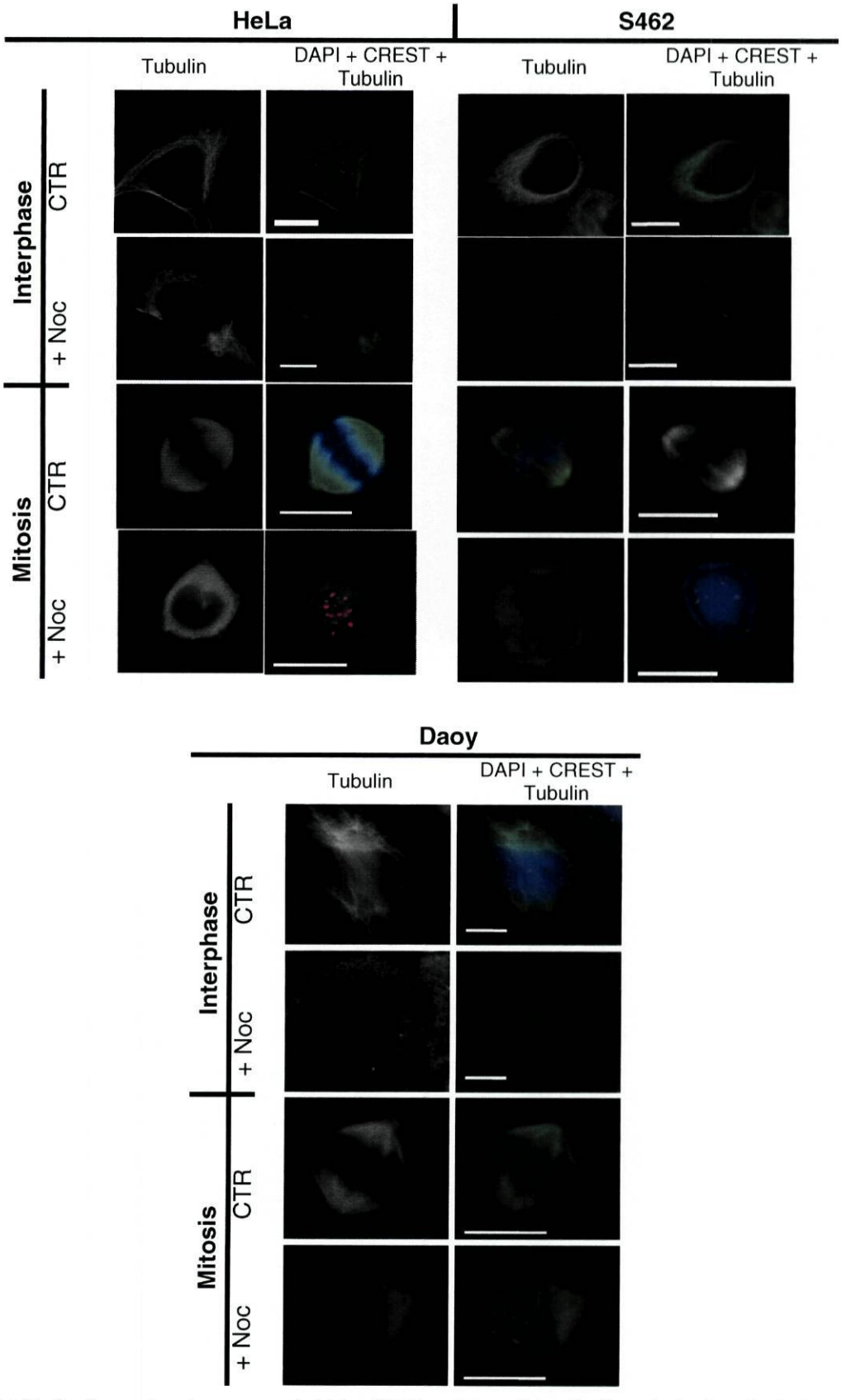

Fig. 3.1: Effects of nocodazole exposure in HeLa, S462 and Daoy interphasic and mitotic cells. In the controls (CTR), no nocodazole was added. Interphasic and mitotic cells were observed under fluorescence microscopy. Independently of the cell cycle phase, microtubules appear correctly assembled in the absence of the drug, while in its presence they are depolymerised. DNA is shown in blue, α-tubulin in green and CREST in red. Scale bars, 5 μm.

As shown in **figure 3.1**, in the absence of nocodazole (CTR), interphase cells show a well-defined microtubule net and these compose a functional, bipolar spindle in mitotic cells, as expected. However, microtubules become depolymerised in the three cell lines after nocodazole treatment. These observations indicate that cells metabolise the drug and that any change in their behaviour upon exposure to it is not due to any kind of nocodazole rejection mechanism. As a result of nocodazole action, mitotic spindle assembly is prevented; chromosome capture and congression (and, consequently, alignment at the metaphase plate) are thus inhibited. Mitotic progression is compromised and cell division can no longer take place.

3.1.1 Daoy cell line exhibits a low mitotic index upon nocodazole exposure

Because microtubule depolymerisation compromises spindle assembly and generates unattached kinetochores that are sensed by the mitotic checkpoint, and once it was shown to occur in Daoy cells when these are exposed to nocodazole, incubation with the drug was expected to induce a mitotic arrest and, consequently, an increase in mitotic index. Cells were therefore incubated with nocodazole for distinct periods of time. In each of them, mitotic index was determined in three independent experiments. The same procedure was done in the control cultures, but with no nocodazole addition. The mean values are depicted in **fig. 3.2**.

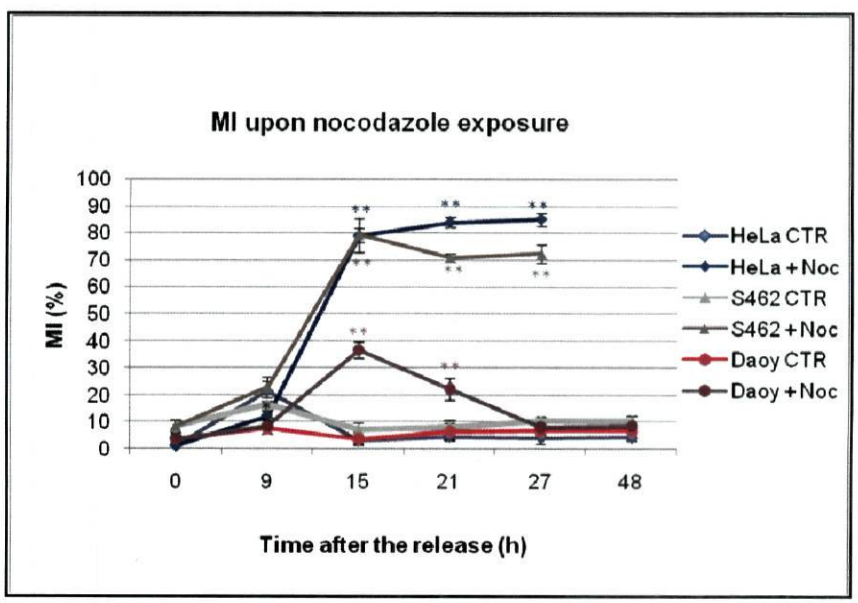

Fig. 3.2: Mitotic index (MI) from HeLa, S462 and Daoy cell cultures treated with nocodazole (+ Noc). In the controls (CTR), no nocodazole was added. Data are mean ± S.D. (n = 3 independent experiments). * $p<0.05$; ** $p<0.01$.

When compared with control HeLa cells, Daoy control cells show slightly higher (but comparable) mitotic index values (~7% versus ~5%), except for the immediate hours after the release, in which there is a greater percentage of HeLa mitotic cells (~20% versus ~7%). S462 cells, in turn, are those that exhibit the highest mitotic index values in the absence of nocodazole (~10%), also achieving a peak value in the first 9 hours of the release (~17%). The differences in mitotic index values observed between the three control situations may be justified by their distinct proveniences (HeLa, cervical cancer; Daoy, medulloblastoma; S462, malignant peripheral nerve sheath tumour).

Concerning the situations where nocodazole was added, it can be stated that HeLa and S462 cells accumulate in mitosis, as expected considering nocodazole action, and eventually die as a consequence of a prolonged arrest in prometaphase. In effect, a pronounced increase in the number of mitotic cells is seen early in response to nocodazole addition, with mitotic index values rising in the first 6 hours of incubation and peaking about 15 hours after the release (that is to say, 12 hours upon nocodazole addition), both presenting 80% mitotic cells. Mitotic index values close to this were again obtained upon 19 and 24 hours of exposure but were no longer determined from this moment on because, at about this time, these cells begin to die. The results are in agreement with the known efficient mitotic checkpoint in HeLa cells and show that S462 cells also have an efficient mitotic checkpoint.

On the contrary, although Daoy cells do accumulate in mitosis – as it can be deduced from the MI peak value reached at about 15 hours after the release (36.1%, a statistically significant different value from the control culture) –, this increase in their mitotic index is much more subtle than in HeLa and S462 cases (which achieve ~85% and 70% mitotic index values, respectively). Then, instead of stabilising its mitotic values and eventually dying, the number of Daoy mitotic cells actually decreases because they escape mitosis – as confirmed by the presence of many normal looking interphase cells (**fig. 3.3**) –, even after prolonged incubation with the drug. In fact, after 45 hours of exposure, cells at different cell cycle phases are observed (data not shown). We observed few Daoy dead cells in the presence of nocodazole, which is consistent with the presence of a defective mitotic checkpoint in this cell line.

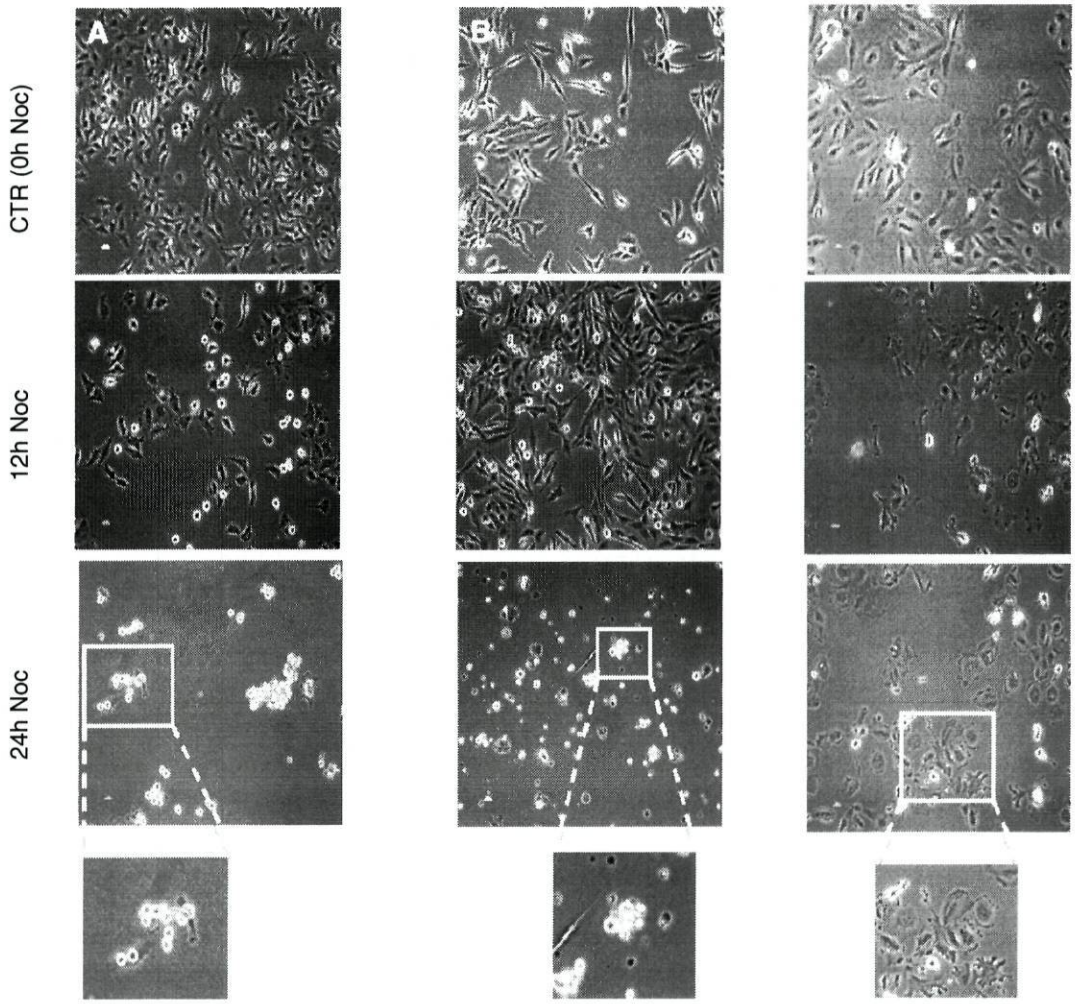

Fig. 3.3: Nocodazole effects along with time in synchronized HeLa (**A**), S462 (**B**) and Daoy (**C**) cell cultures. Phase contrast images (40× magnification) show cell cultures upon a 12 and a 24-hour exposure period to nocodazole (Noc), as well as the corresponding controls (CTR). Incubation with nocodazole results in significant differences in the number of mitotic and interphasic cells between the three cell lines. Upon 24 hours of incubation, while HeLa and S462 cultures are arrested in mitosis and start to evidence signals of cell death, Daoy cultures present colonies of interphasic cells, with a low number of mitotic cells.

3.1.2 Chromosome spread assays

In order to verify to which extent sister chromatids remained held together during the prolonged mitotic arrest, chromosome spread assays were performed (Maraldi *et al.*, 1999). As shown in **fig. 3.4A** and as expected, HeLa and S462 sister chromatids remain held together during nocodazole-induced mitotic arrest. Nonetheless, Daoy cells show a high number of mitosis-arrested cells with sister chromatid separation (SCS).

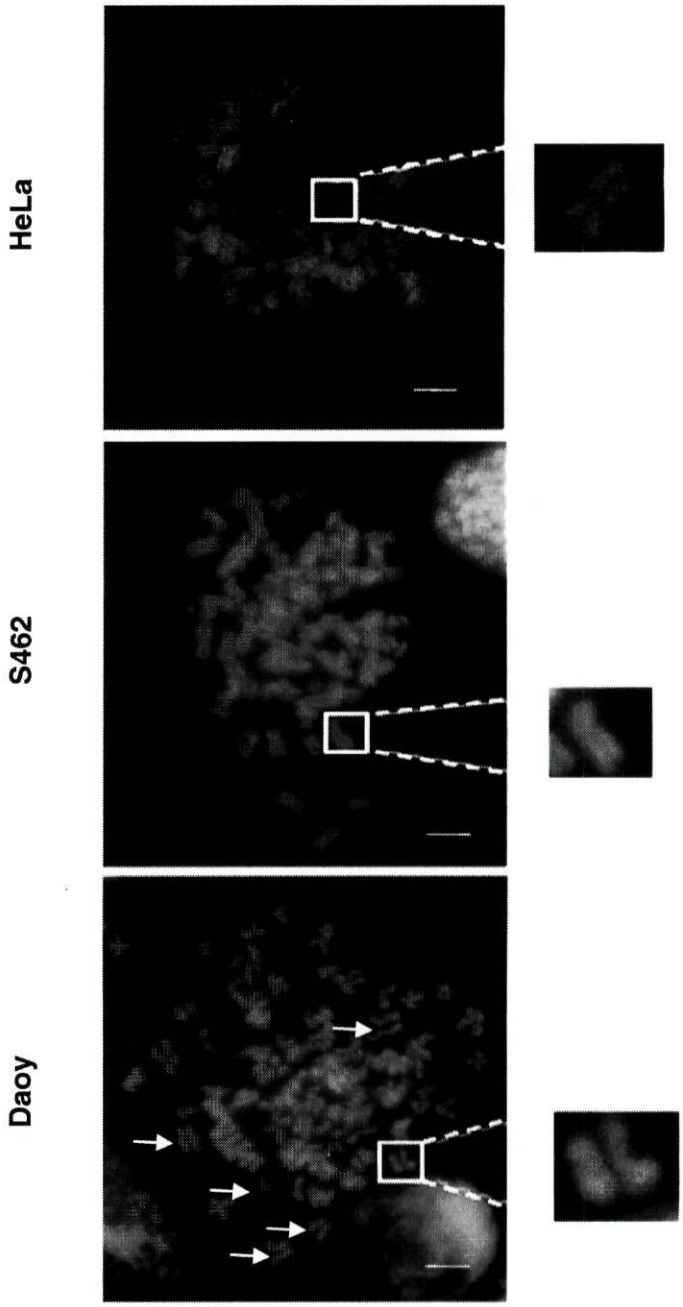

Fig. 3.4A: Chromosome spread results in HeLa, S462 and Daoy cell lines upon an 8 hour-exposure to 0.5 µM nocodazole. In the presence of the drug, sister chromatids remain held together at the centromere in HeLa and S462 mitosis-arrested cells. On the contrary, there is a significant number of mitotic cells showing separated sister chromatids (white arrows) in the Daoy cell line. A magnification of a representative chromosome is provided for each cell line. Scale bars, 5 µm.

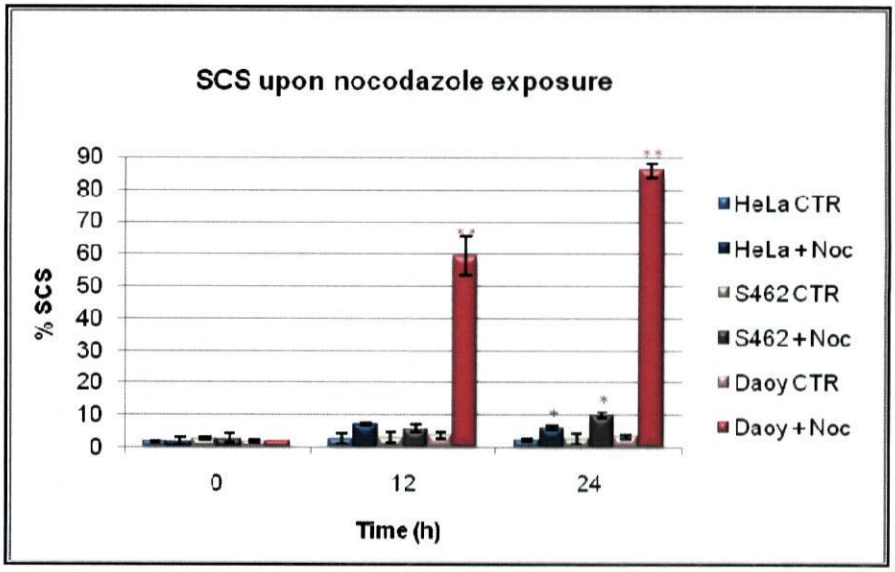

Fig. 3.4B: Percentage of sister chromatid separation (% SCS) in HeLa, S462 and Daoy cell cultures upon a 0, 12- and 24-hour period of incubation with 0.5 μM nocodazole (+ Noc). Data are mean ± S.D. (*n* = 3 independent experiments). * $p<0.05$; ** $p<0.01$.

Fig. 3.4B depicts that, in HeLa and in S462 cells, a very low number of mitotic cells presented sister chromatid separation (SCS) in the absence of nocodazole (1.9% in HeLa and 2.7% in S462 cells), which also did not increase significantly in the presence of the drug upon 12 hours of exposure (7.3% and 5.8% of SCS in HeLa and in S462 cells, respectively).

On the contrary, Daoy cells showed a steep increase in the percentage of cells with SCS during incubation with nocodazole. At 0h, Daoy SCS percentage values were comparable to those from HeLa and S462 cell lines (2.0%), but the frequency of cells with SCS rose remarkably in the presence of nocodazole (59.5% and 85.8% of the cells showed SCS after 12 and 24 hours of incubation with the drug, respectively).

Therefore, in spite of being arrested in mitosis, as judged by phase contrast microscopy observation, a high percentage of Daoy cells presents sister chromatid separation. These results are consistent with a defective mitotic checkpoint in Daoy cells.

3.2 Mitotic checkpoint proteins exhibit a normal subcellular distribution in the Daoy cell line

Once spindle assembly checkpoint was proven to be defective in Daoy cells, the study was directed towards the analysis of specific checkpoint proteins, so as to establish a molecular explanation for the observed defects. In a first approach, in order to qualitatively verify protein cellular localisation and to monitor it along with mitosis progression, different mitotic proteins were labelled by immunofluorescence in HeLa, S462 and Daoy cell cultures. **Fig. 3.5** and **fig. 3.6**, respectively, show Bub1 and BubR1 subcellular localisations in different mitosis stages.

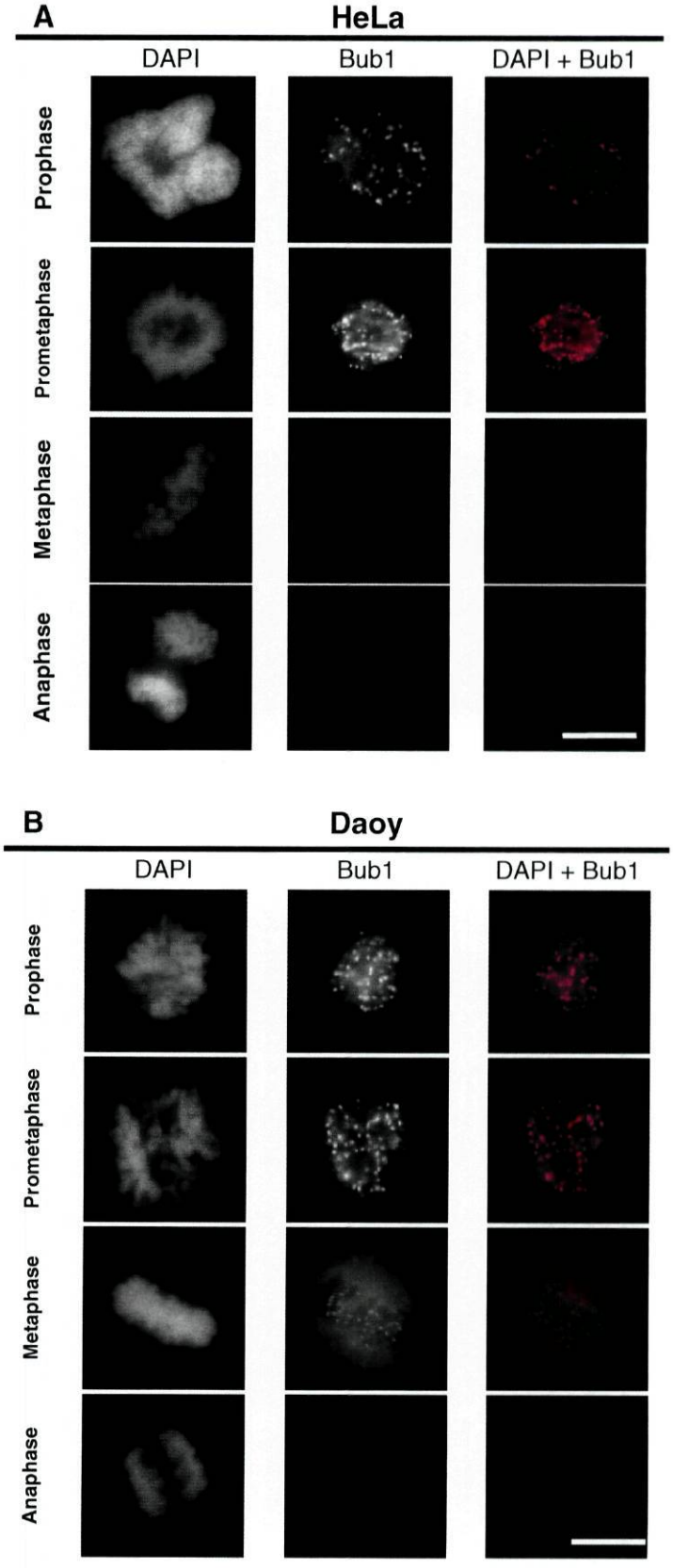

Fig. 3.5: Bub1 intracellular distribution patterns in HeLa (**A**) and Daoy (**B**) cells throughout mitosis. Bub1 is shown in red. DNA was stained with DAPI (blue). Immunofluorescence images show that Bub1 concentrates at kinetochores during prophase and prometaphase and decreases significantly at metaphase and anaphase. The same spatial and temporal distribution is observed in both cell lines. Scale bars, 5 µm.

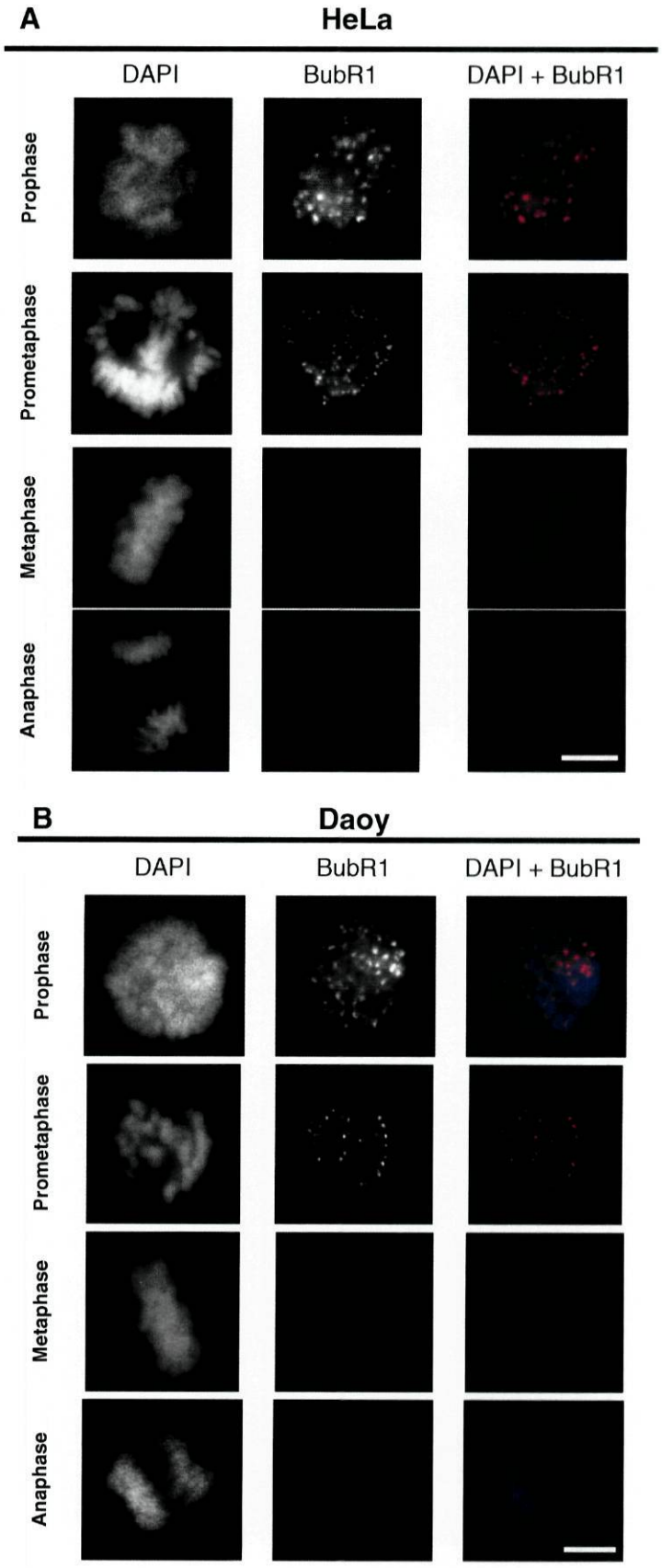

Fig. 3.6: BubR1 intracellular distribution patterns in HeLa (**A**) and Daoy (**B**) cells throughout mitosis. BubR1 is shown in red. DNA was stained with DAPI (blue). Immunofluorescence images show that BubR1 concentrates at kinetochores during prophase and prometaphase and decreases significantly at metaphase and anaphase. The same spatial and temporal distribution is observed in both cell lines. Scale bars, 5 µm.

For these proteins, the same subcellular and temporal distribution patterns were observed. In both cell lines, as well as in S462 cells (data not shown), this distribution is in accordance with the reported for these proteins. In effect, Bub1 and BubR1 were shown to localise to kinetochores, to accumulate during prophase and prometaphase, to have a diminished signal in metaphase and to be undetectable in anaphase, which coincides with their predictable temporal behaviour while mitotic proteins (Clarke and Giménez-Abián, 2000).

The fact that no detectable changes were observed between control cell lines and Daoy cells suggests that eventual alterations in spatial and temporal distribution of mitotic checkpoint proteins do not lie beneath the evident defects of its activity.

3.3 Daoy cell line shows altered expression of mitotic checkpoint genes

Besides analysing the intracellular and temporal distribution of mitotic checkpoint proteins, the present work also focused on the study of their expression, at the gene and protein levels, in order to find a molecular explanation for the observed mitotic checkpoint defects. To do so, protein expression levels were assessed by Western blotting and the corresponding gene expression levels were evaluated by quantitative Real-Time PCR.

In Western blotting assays, total protein extracts prepared from HeLa, S462 and Daoy cell cultures exposed to 0.5 μM nocodazole for 16 hours were used along with the corresponding controls. Bub1, BubR1, Bub3 and α-tubulin were labelled; α-tubulin was used as loading control (**fig. 3.7**).

Cell line	HeLa		S462		Daoy		Molecular weight (kDa)	Daoy protein expression levels (%)	
Nocodazole	-	+	-	+	-	+		Relative to HeLa	Relative to S462
Bub1							122	85	65
α-Tubulin							55		
BubR1							120	90	82
α-Tubulin							55		
Bub3							37	87	98
α-Tubulin							55		

Fig. 3.7: Western blots concerning Bub1, BubR1 and Bub3 protein expression levels in HeLa, S462 and Daoy cell lines growing in the presence (+) or in the absence (-) of 0.5 μM nocodazole for 16 hours. Total protein extracts were harvested, separated on 10% (Bub1 and BuR1) or 15% SDS-PAGE (Bub3), transferred to nitrocellulose membranes and immunoblotted using anti-Bub1, anti-BubR1, anti-Bub3 and anti-α-tubulin antibodies. α-Tubulin was used as loading control. Bub1, BubR1 and Bub3 protein levels in cell cultures growing in the absence of nocodazole were determined by densitometry and expressed relative to HeLa and S462 control cultures.

As far as Bub3 protein expression levels are concerned, there were no significant changes between the three cell lines, with the intensities of α-tubulin-corresponding bands dissuading any apparent differences.

In turn, analysis of the Bub1 and BubR1 blots reveals that, in HeLa and S462 cell lines, the levels of expression of these proteins are higher, either in the presence or in the absence of nocodazole. Furthermore, it must be emphasized that, in the situations where the drug was added, Bub1 and BubR1 bands are more intense in HeLa and S462, which was already expected since these are mitotic proteins, thereby accumulating in conditions in which a mitotic arrest is induced. Since these cells have a very efficient response to nocodazole and markedly arrest at mitosis, their amount is consequently higher in HeLa and S462 cells than in those from the Daoy cell line, which accumulate less in mitosis. In fact, Daoy lower levels of expression of Bub1 and BubR1 as a consequence of a weaker mitotic arrest in the presence of the microtubule disruptor corroborate the results obtained in mitotic index determinations, which have shown that these cells accumulate in mitosis

to a lesser extent when compared with those from HeLa and S462 lines in the same conditions.

Differences in band intensities of mitotic checkpoint proteins found through Western blotting assays led to the hypothesis that their expression levels are altered in Daoy cells. In order to confirm this suspicion, their corresponding mRNA levels were assessed through Real-Time PCR. Mad2, Bub1, BubR1, Bub3, Cdc20 and Chfr gene expression levels were studied in this context.

Gene expression analysis by means of Real-Time PCR made use of appropriate primer pairs, whose specificity was confirmed in a preliminary PCR assay. This experiment has proven that each primer pair amplified a single fragment. Total RNA samples were isolated from HeLa, S462 and Daoy cell lines growing in the absence of nocodazole; an additional astrocyte total RNA sample, prepared in the same conditions, was also included in the assays. Astrocyte expression levels were used as controls for the normalization of gene expression since astrocytes are normal glial cells, derived from the brain and spinal cord, having thus a closer provenience to Daoy cells than those from HeLa (which derive from cervical cancer). The use of astrocyte expression levels as controls eliminates the differences in gene expression arising from distinct cell line origins. Also, gene expression levels were normalized against those of GAPDH, a housekeeping gene whose expression did not vary between the cell lines used under our experimental conditions.

Analysis of Real-Time PCR results reveals statistically significant differences in the expression levels of all the genes that were tested except for Bub1. In effect, Mad2, BubR1 and Bub3 genes are underexpressed in Daoy cells, whilst Cdc20 is overexpressed (**fig. 3.8**).

In Daoy cells, Bub1 gene was found to be only 5% less expressed than in astrocytes, a little divergence that is not statistically different and, therefore, not considered as an underexpression. In fact, all four cell lines showed comparable values of Bub1 expression levels. However, if compared to those of HeLa, Daoy Bub1 expression levels are more underexpressed, in accordance to what has been observed in the analysis of protein expression through Western blotting (**fig. 3.7**).

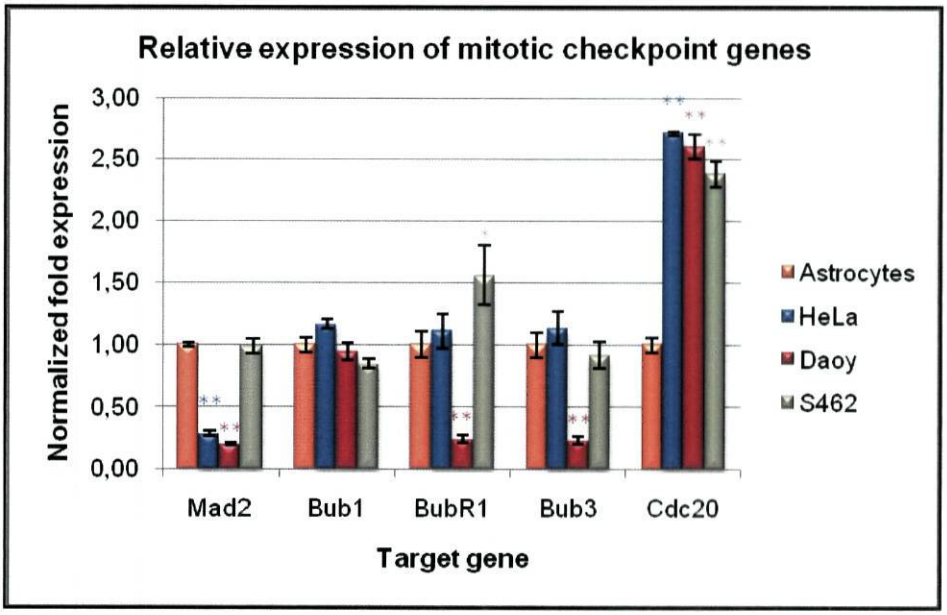

Fig. 3.8: Relative mean expression levels of Mad2, Bub1, BubR1, Bub3 and Cdc20 genes in astrocyte, HeLa, Daoy and S462 cell lines. Expression levels were normalized against those of the housekeeping gene GAPDH; the resulting values were normalized against those from astrocytes, which were established as 1.00 (100%). Mad2, BubR1 and Bub3 genes are underexpressed in Daoy cells, while that of Cdc20 is overexpressed. Data are mean ± S.D. (n = 3 independent experiments). * $p<0.05$; ** $p<0.01$.

Mad2 encoding gene, in turn, was found to be pronouncedly underexpressed, with an 80% reduction in its expression levels relative to astrocytes. Similarly, Daoy cell line was demonstrated to express only 25% and 23% of BubR1 and Bub3 astrocyte levels (defined as 100%), respectively. Again, if compared with HeLa expression levels, BubR1 is underexpressed in the Daoy cell line, in compliance with what has been observed when the corresponding protein levels were studied by means of Western blotting (**fig. 3.7**). A relevant finding was that S462 cells have a 46% higher BubR1 gene expression level relative to that of HeLa cells, an overexpression that is also substantiated by the corresponding Western blotting results (**fig. 3.7**).

On the other hand, Cdc20 gene was shown to be overexpressed in Daoy cells, where its expression levels are equivalent to 261% of those of astrocytes. High levels of Cdc20, the essential component for APC/C activity, contribute to premature metaphase-to-anaphase transitions, propitiating the occurrence of abnormal chromosome segregation and leading to aneuploidy (Schmidt and Medema, 2006), which may explain why Daoy cells prematurely exit from mitosis even in the presence of the mictotubule-depolymerising drug.

Besides investigating the expression levels of genes encoding for mitotic checkpoint proteins that act specifically at the metaphase-to-anaphase transition, the

present study did also comprise the analysis of Chfr gene expression (**fig. 3.9**). Although it was also shown to play a role later in mitosis, having been implied in events such as spindle formation, chromosome segregation, and even in the mitotic checkpoint, Chfr was primordially reported to intervene in late G2, delaying prophase in case of mitotic stress (Scolnick and Halazonetis, 2000; Chaturvedi *et al.*, 2002; Gong, 2004; Loring *et al.*, 2008; Privette and Petty, 2008). It therefore constitutes an important control point for the cell cycle to advance into mitosis. Real-Time PCR assays demonstrated an overexpression of Chfr gene in Daoy cells, in which it is 9.52 times more expressed than in astrocytes. In the S462 cell line, this gene is 12 times more expressed than in astrocytes (**fig. 3.9**).

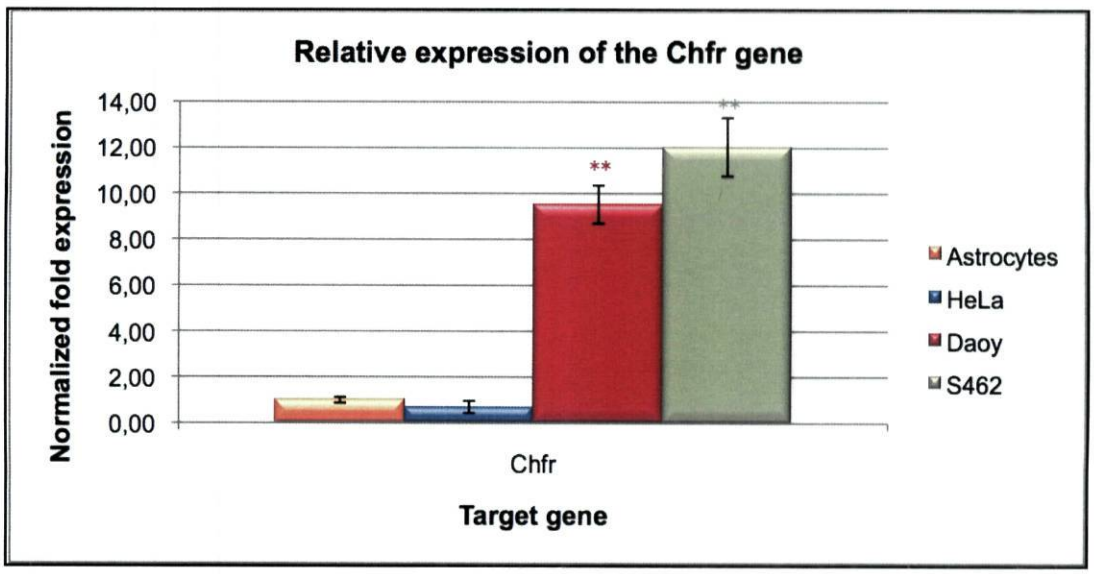

Fig. 3.9: Relative mean expression levels of the Chfr gene in astrocyte, HeLa, Daoy and S462 cell lines. Expression levels were normalized against those of the housekeeping gene GAPDH; the resulting values were normalized against those from astrocytes, which were established as 1.00 (100%). Chfr is overexpressed in Daoy cells. Data are mean ± S.D. (n = 3 independent experiments). ** $p<0.01$.

Taken together, the results demonstrate that, in spite of being present in these cells, the spindle assembly checkpoint works defectively. A compensatory molecular mechanism, through which overexpression of some proteins may compensate for the underexpression of others, may constitute the reason why it partially maintains its function without compromising tumour cell viability. For instance, Chfr gene overexpression may represent a compensatory mechanism responsible for keeping genetically abnormal cells, which result from failures in the mitotic checkpoint activity, from advancing into another mitosis.

Loss-of-function mutations of genes of the spindle checkpoint machinery are rare in solid tumours; other mechanisms such as deregulated expression are speculated to underlie chromosomal instability (Hernando *et al.*, 2001; Saeki *et al.*, 2002; Rimkus *et al.*,

2004; Schmidt and Medema, 2006). Given mitotic checkpoint proteins' crucial role for proper mitotic divisions – and, among these, Bub and Mad family proteins' role in particular –, any alteration in their expression levels may seriously compromise their functions and, therefore, an adequate chromosomal segregation (May and Hardwick, 2006; Musacchio and Salmon, 2007).

The alterations that were detected in mitotic gene and protein expression may explain, at least in part, mitotic checkpoint inefficiency observed in the Daoy cell line. In addition, they may account for medulloblastoma pathogenesis and contribute to its proliferation and malignancy.

4. Conclusions

Sister chromatid segregation is a complex process whose accuracy, as a prerequisite for genetic stability, is dependent on the activity of the mitotic checkpoint. In particular, Bub and Mad family proteins have been shown to be crucial for mitotic checkpoint functions (May and Hardwick, 2006; Musacchio and Salmon, 2007). Defects in its mechanism are responsible for unequal chromosome partitioning between daughter cells and, consequently, for loss or gain of chromosomes during cell divisions. The resulting genetic imbalance, known as aneuploidy, is a hallmark of cancer cells (Bharadwaj and Yu, 2004; Kops *et al.*, 2005; Sengupta *et al.*, 2007). Although mutations in genes encoding for checkpoint proteins are rare, alterations in their expression levels have been reported in several works and are thought to be the actual cause of karyotypic abnormalities observed in cancer cells (Hernando *et al.*, 2001; Saeki *et al.*, 2002; Rimkus *et al.*, 2004; Schmidt and Medema, 2006).

Medulloblastoma, the most frequent brain tumour in childhood, is a highly malignant neoplasm with a poor prognosis in the vast majority of cases. Current treatment methods combine surgical resection and chemotherapy, which impair physical and cognitive development. Besides presenting chromosome structural and numerical aberrations (Wechsler-Reya, 2003; De Smaele *et al.*, 2004; Ferretti *et al.*, 2005), mutations in elements of the Shh-Ptch and Wnt pathways, both involved in cell development and proliferation, are documented in different works with medulloblastoma cells (Wechsler-Reya, 2003; Collins, 2004; Pogoriler, 2006).

The present work aimed at studying the competence of the mitotic checkpoint in a medulloblastoma cell line – Daoy –, as well at characterizing the subjacent molecular alterations.

Our results show that: **(1)** Daoy cells do have a mitotic checkpoint, but it works defectively, as demonstrated by their low mitotic index and their ability to escape mitosis without apoptosis upon incubation with microtubule-disrupting drugs; **(2)** The mitotic checkpoint proteins have a normal temporal and spatial distribution in Daoy cells; **(3)** The mitotic checkpoint genes have altered expression both at protein and mRNA levels. More specifically, BubR1, Bub3 and Mad2 were shown to be underexpressed, while Cdc20 and Chfr were shown to be overexpressed.

Although the mechanisms underlying improper chromosomal segregation and aneuploidy are not yet completely established, our results have demonstrated that mitotic checkpoint competence is compromised in the medulloblastoma cell line under analysis and that alterations in the expression of mitotic checkpoint genes may lie behind the observed checkpoint inefficiency and contribute to medulloblastoma pathogenesis and/or progression. A complete understanding of the mitotic checkpoint mechanism and of the molecular basis underlying its defects in medulloblastomas may hold the key for a novel strategy for their therapy.

5. Future Prospects

It would be suitable to include, in all experimental studies, a primary, normal cell line having the same origin as that of medulloblastomas, an internal control that would allow a more direct comparison of the results and legitimate a more immediate validation of those obtained with Daoy cells. This strategy has actually been followed in the Real-Time PCR experiments, where RNA from normal astrocytes has been used. Nevertheless, because the astrocyte cell line itself was not available in the laboratory, it was not possible to contemplate it in the phenotypic studies presented for HeLa, S462 and Daoy cell lines. Furthermore, it would be interesting to include astrocyte protein extracts in the Western blotting assays, in order to ascertain whether protein expression levels reflect gene expression tendencies observed in Real-Time PCR results.

In addition, since Real-Time PCR and Western blotting assays have consistently shown that, in Daoy cells, some spindle assembly checkpoint genes are underexpressed, while others are overexpressed, it would be interesting to interfere with the expression of these genes so as to study the corresponding effects on cell proliferative activity and survival. Cell line transfection with expression recombinant vectors would allow the evaluation of protein overexpression effects on mitotic checkpoint activity in the tumour cell lines under study and the analysis of the overexpression of some proteins as a means to compensate for the underexpression of others. Conversely, expression levels of overexpressed proteins could be lowered by means of RNAi-mediated gene knockdown in order to understand how important the overexpression of these genes is to tumour cell proliferation and survival.

Since mitotic checkpoint proteins' functions are dependent on the interactions they establish with each other and with other proteins, this study should be broadened in order to include a greater number of mitotic checkpoint-related proteins, aiming at characterizing their distribution and expression in the cell lines under analysis. This would provide a wider perspective over the molecular interactions, defects and possible compensatory mechanisms developed by tumour cells in order to develop, tolerate and proliferate while harbouring aneuploidy.

It is also necessary to repeat the experiments done so far with the Daoy medulloblastoma cell line with tissue samples from medulloblastoma patients, with which immunohistochemical assays may be done in order to compare *in vitro* results with those obtained *in vivo*.

6. References

- Abal M, Obrador-Hevia A, Janssen KP, Casadome L, Menendez M, Carpentier S, Barillot E, Wagner M, Ansorge W, Moeslein G, Fsihi H, Bezrookove V, Reventos J, Louvard D, Capella G, Robine S (2007). APC inactivation associates with abnormal mitosis completion and concomitant BUB1B/MAD2L1 up-regulation. *Gastroenterology* 132(7): 2448-58.

- Aguilera A, Gómez-González B (2008). Genome instability: a mechanistic view of its causes and consequences. *Nat Rev Genet* 9: 204-217.

- Berghmans S, Murphey RD, Wienholds E, Neuberg D, Kutok JL, Fletcher CD, Morris JP, Liu TX, Schulte-Merker S, Kanki JP, Plasterk R, Zon LI, Look AT (2005). tp53 mutant zebrafish develop malignant peripheral nerve sheath tumors. *Proc Natl Acad Sci USA* 102(2): 407-412.

- Bharadwaj R, Yu H (2004). The spindle checkpoint, aneuploidy, and cancer. *Oncogene* 23: 2016-2027.

- Chan GK, Liu S-T, Yen TY (2005). Kinetochore structure and function. *TRENDS in Cell Biology* 15(11): 589-598.

- Chaturvedi P, Sudakin V, Bobiak ML, Fisher PL, Mattern MR, Jablonski SA, Hurle MR, Zhu Y, Yen TJ, Zhou B-BS (2002). Chfr regulates a mitotic stress pathway through its RING finger domain with ubiquitin ligase activity. *Cancer Res* 62: 1797-1801.

- Cheeseman IM, Desai A (2008). Molecular architecture of the kinetochore-microtubule interface. *Nat Rev Mol Cell Biol* 9: 33-46.

- Clarke DJ, Giménez-Abián JF (2000). Checkpoints controlling mitosis. *BioEssays* 22: 351-363.

- Collins VP (2004). Brain tumours: classification and genes. *J Neurol Neurosurg Psychiatry* 75(Suppl 2): ii2-ii11.

- Compton DA (2000). Spindle assembly in animal cells. *Annu Rev Biochem* 69: 95:114.

- Corn PG, Summers MK, Fogt F, Virmani AK, Gazdar AF, Halazonetis TD, El-Deiry WS (2003). Frequent hypermethylation of the 5' CpG island of the mitotic stress checkpoint gene *Chfr* in colorectal and non-small cell lung cancer. *Carcinogenesis* 24(1): 47-51.

• Crasta K, Lim HH, Giddings TH Jr, Winey M, Surana U (2008). Inactivation of Cdh1 by synergistic action of Cdk1 and polo kinase is necessary for proper assembly of the mitotic spindle. *Nat Cell Biol* 10(6): 665-675.

• Cuomo ME, Knebel A, Morrice N, Paterson H, Cohen P, Mittnacht S (2008). p53-Driven apoptosis limits centrosome amplification and genomic instability downstream of NPM1 phosphorylation. *Nature Cell Biology* 10(6): 723-730.

• De Smaele E, Di Marcotullio L, Ferretti E, Screpanti I, Alesse E, Gulino A (2004). Chromosome 17p deletion in human medulloblastoma: a missing checkpoint in the Hedgehog pathway. *Cell Cycle* 3(10):1263-1266.

• Doxsey S, Zimmerman W, Mikule K (2005). Centrosome control of the cell cycle. *Trends Cell Biol* 15(6): 303-311.

• Earnshaw WC, Mackay AM (1994). Role of nonhistone proteins in the chromosomal events in mitosis. *FASEB J* 8: 947-956.

• Egozi D, Shapira M, Paor G, Ben-Izhak O, Skorecki K, Hershko DD (2007). Regulation of the cell cycle inhibitor p27 and its ubiquitin ligase Skp2 in differentiation of human embryonic stem cells. *The FASEB Journal* 21: 2807-2817.

• Ferretti E, De Smaele E, Di Marcotullio L, Screpanti I, Gulino A. (2005) Hedgehog checkpoints in medulloblastoma: the chromosome 17p deletion paradigm. *Trends Mol Med* 11(12): 537-545.

• Gadde S, Heald R (2004). Mechanisms and molecules of the mitotic spindle. *Curr Biol* 14(18): R797-805.

• Garrett MD (2001). Cell cycle control and cancer. *Current Science* 81(5): 515-522.

• Grabsch HI, Askham JM, Morrison EE, Pomjanski N, Lickvers K, Parsons WJ, Boecking A, Gabbert HE, Mueller W (2004). Expression of BUB1 protein in gastric cancer correlates with the histological subtype, but not with DNA ploidy or microsatellite instability. *J Pathol* 202(2): 208-14.

• Grabsch H, Takeno S, Parsons WJ, Pomjanski N, Boecking A, Gabbert HE, Mueller W (2003). Overexpression of the mitotic checkpoint genes BUB1, BUBR1, and BUB3 in gastric cancer – association with tumour cell proliferation. *J Pathol* 200(1): 16-22.

◆ Gurney JG, Smith MA, Bunin GR (2000). CNS and miscellaneous intracranial and intraspinal neoplasms. In *SEER Pediatric Monograph* http://seer.cancer.gov/Publications, National Cancer Institute: 51-63.

◆ Hauf S, Watanabe Y (2004). Kinetochore orientation in mitosis and meiosis. *Cell* 119: 317-327.

◆ Hernando E, Orlow I, Liberal V, Nohales G, Benezra R, Cordon-Cardo C (2001). Molecular analyses of the mitotic checkpoint components hsMAD2, hBUB1 and hBUB3 in human cancer. *Int J Cancer* 95(4): 223-227.

◆ Howell BJ, McEwen BF, Canman JC, Hoffman DB, Farrar EM, Rieder CL, Salmon ED (2001). Cytoplasmic dynein/dynactin drives kinetochore protein transport to the spindle poles and has a role in mitotic spindle checkpoint inactivation. *J Cell Biol* 155: 1159-1172.

◆ Hoyt MA (2001). A new view of the spindle checkpoint. *The Journal of Cell Biology* 154(5): 909-911.

◆ Kang D, Chen J, Wong J, Fang G (2002). The checkpoint protein Chfr is a ligase that ubiquitinates Plk1 and inhibits Cdc2 at the G2 to M transition. *The Journal of Cell Biology* 156(2): 249-259.

◆ Kar M, Deo SVS, Shukla NK, Malik A, DattaGupta S, Mohanti BK, Thulkar S (2006). Malignant Peripheral Nerve Sheath Tumours (MPNST) – Clinicopathological study and treatment outcome of twenty-four cases. *World J Surg Oncol* 4:55.

◆ Karess R (2005). Rod-Zw10-Zwilch: a key player in the spindle checkpoint. *Trends Cell Biol* 15: 386-392.

◆ Kaufmann WK, Paules RS (1996). DNA damage and cell cycle checkpoints. *The FASEB Journal* 10: 238-247.

◆ Kawabe T (2004). G_2 checkpoint abrogators as anticancer drugs. *Mol Cancer Ther* 3(4): 513-519.

◆ Kobayashi C, Oda Y, Takahira T, Izumi T, Kawaguchi K, Yamamoto H, Tamiya S, Yamada T, Iwamoto Y, Tsuneyoshi M (2006). Aberrant expression of CHFR in malignant peripheral nerve sheath tumors. *Mod Pathol* 19(4): 524-532.

◆ Kops GJPL, Weaver BAA, Cleveland DW (2005). On the road to cancer: aneuploidy and the mitotic checkpoint. *Nat Rev Cancer* 5: 773-785.

• Kwon M, Godinho SA, Chandhock NS, Ganem NJ, Azioune A, Thery M, Pellman D (2008). Mechanisms to suppress multipolar divisions in cancer cells with extra centrosomes. *Genes Dev* 22: 2189-2203.

• Lew DJ, Burke DJ (2003). The spindle assembly and spindle position checkpoints. *Annu Rev Genet* 37: 251-282.

• Lewin B (2004). Genes VIII. *Pearson Prentice Hall*, Upper Saddle River, NJ: 843-937.

• Li Y, Lal B, Kwon S, Fan X, Saldanha U, Reznik TE, Kuchner EB, Eberhart C, Laterra J, Abounader R (2005). The scatter factor/hepatocyte growth factor: c-met pathway in human embryonal central nervous system tumor malignancy. *Cancer Res.* 65(20): 9355-9362.

• Lodish H, Berk A, Zipursky SL, Matsudaira P, Baltimore D, Darnell JE (2000). Molecular Cell Biology – 4th edition. WH Freeman and Company, New York.

• Logarinho E, Bousbaa H (2008). Kinetochore-microtubule interactions "in check" by Bub1, Bub3 and BubR1 – The dual task of attaching and signalling. *Cell Cycle* 7(12): 1763-1768.

• Logarinho E, Resende T, Torres C, Bousbaa H (2008). The human spindle assembly checkpoint protein Bub3 is required for the establishment of efficient kinetochore-microtubule attachments. *Molecular Biology of the Cell* 19: 1798-1813.

• Loring GL, Christensen KC, Gerber SA, Brenner C (2008). Yeast Chfr homologs retard cell cycle at G1 and G2/M *via* Ubc4 and Ubc13/Mms2-dependent ubiquitination. *Cell Cycle* 7(1): 96-105.

• Maiato H, DeLuca J, Salmon ED, Earnshaw WC (2004). The dynamic kinetochore-microtubule interface. *Journal of Cell Science* 117: 5461-5477.

• Mantel C, Guo Y, Lee MR, Kim M-K, Han M-K, Shibayama H, Fukuda S, Yoder MC, Pelus LM, Kim K-S, Broxmeyer HE (2007). Checkpoint-apoptosis uncoupling in human and mouse embryonic stem cells: a source of karyotpic instability. *Blood* 109: 4518-4527.

• Mapelli M, Filipp FV, Rancati G, Massimiliano L, Nezi L, Stier G, Hagan RS, Confalonieri S, Piatti S, Sattler M, Musacchio A (2006). Determinants of conformational dimerization of Mad2 and its inhibition by p31^{comet}. *EMBO J* 25(6): 1273-1284.

• Maraldi NM, Capitani S, Cinti C, Neri LM, Santi S, Squarzoni S, Stuppia L, Manzoli FA (1999). Chromosome spread for confocal microscopy. *Methods Enzymol* 307: 190-207.

• Marangos P, Carroll J (2008). Securin regulates entry into M-phase by modulating the stability of cyclin B. *Nat Cell Biol* 10: 445-451.

• May KM, Hardwick KG (2006). The spindle checkpoint. *Journal of Cell Science* 119: 4139-4142.

• McGowan CH (2003). Regulation of the eukaryotic cell cycle. *Progress in Cell Cycle Research* 5: 1-4.

• Morgan DO (1999). Regulation of the APC and the exit from mitosis. *Nat Cell Biol* 1: E47-53.

• Murray AW (2004). Recycling the cell cycle: cyclins revisited. *Cell* 116: 221-234.

• Musacchio A, Salmon ED (2007). The spindle-assembly checkpoint in space and time. *Nature Reviews – Molecular Cell Biology* 8: 379-393.

• Nasmyth K (2005). How do so few control so many? *Cell* 120(6): 739-746.

• Nigg EA (2001). Mitotic kinases as regulators of cell division and its checkpoints. *Nature Reviews – Molecular Cell Biology* 2: 21-32.

• Niikura Y, Dixit A, Scott R, Perkins G, Kitagawa K (2007). BUB1 mediation of caspase-independent mitotic death determines cell fate. *The Journal of Cell Biology* 178(2): 283-296.

• Odde DJ (2005). Chromosome capture: take me to your kinetochore. *Curr Biol* 15(9): R328-330.

• Peters JM (2002). The anaphase-promoting complex: proteolysis in mitosis and beyond. *Mol Cell* 9: 931-943.

• Pinsky BA, Biggins S (2005). The spindle checkpoint: tension versus attachment. *TRENDS in Cell Biology* 15(9): 486-493.

• Pogoriler J, Millen K, Utset M, Du W (2006). Loss of cyclin D1 impairs cerebellar development and suppresses medulloblastoma formation. *Development* 133(19): 3929-3937.

• Privette LM, González ME, Ding L, Kleer CG, Petty EM (2007). Altered expression of the early mitotic checkpoint protein, CHFR, in breast cancers: implications for tumour suppression. *Cancer Res* 67(13): 6064-6074.

• Privette LM, Petty EM (2008). CHFR: a novel mitotic checkpoint protein and regulator of tumorigenesis. *Translational Oncology* 1: 57-64.

• Privette LM, Weier JF, Nguyen HN, Yu X, Petty EM (2008). Loss of CHFR in human mammary epithelial cells causes genomic instability by disrupting the spindle assembly checkpoint. *Neoplasia* 10: 643-652.

• Reddy SK, Rape M, Margansky WA, Kirschner MW (2007). Ubiquitination by the anaphase-promoting complex drives spindle checkpoint inactivation. *Nature* 446(7138): 921-925.

• Rieder CL, Schultz A, Cole R, Sluder G (1994). Anaphase onset in vertebrate somatic cells is controlled by a checkpoint that monitors sister kinetochore attachment to the spindle. *The Journal of Cell Biology* 127(5): 1301-1310.

• Rimkus C, Friederichs J, Rosenberg R, Holzmann B, Siewert J-R, Janssen K-P (2006). Expression of the mitotic checkpoint gene *MAD2L2* has prognostic significance in colon cancer. *Int J Cancer* 120: 207-211.

• Saeki A, Tamura S, Ito N, Kiso S, Matsuda Y, Yabuuchi I, Kawata S, Matsuzawa Y (2002). Frequent impairment of the spindle assembly checkpoint in hepatocellular carcinoma. *Cancer* 94(7): 2047-54.

• Schafer KA (1998). The cell cycle: a review. *Vet Pathol* 35: 461-478.

• Schmidt M, Medema RH (2006). Exploiting the compromised spindle assembly checkpoint function of tumor cells – Dawn on the horizon? *Cell Cycle* 5(2): 159-163.

• Schmit TL, Ahmad N (2007). Regulation of mitosis via mitotic kinases: new opportunities for cancer management. *Mol Cancer Ther* 6(7): 1920-1931.

• Scolnick DM, Halazonetis TD (2000). *Chfr* defines a mitotic stress checkpoint that delays entry into metaphase. *Nature* 406: 430-435.

• Sengupta K, Upender MB, Barenboim-Stapleton L, Nguyen QT, Wincovitch SM Sr, Garfield SH, Difilippantonio MJ, Ried T (2007). Artificially introduced aneuploid chromosomes assume a conserved position in colon cancer cells. *PLoS ONE* 2(2): e199.

• Sherr CJ, Roberts JM (1999). CDK inhibitors: positive and negative regulators of G1-phase progression. *Genes Dev* 13: 1501-1512.

• Stegmeier F, Rape M, Draviam VM, Nalepa G, Sowa ME, Ang XL, McDonald 3rd ER, Li MZ, Hannon GJ, Sorger PK, Kirschner MW, Harper JW, Elledge SJ (2007). Anaphase initiation is regulated by antagonistic ubiquitination and deubiquitination activities. *Nature* 446(7138): 876-881.

• Sudakin V, Chan GK, Yen TJ (2001). Checkpoint inhibition of the APC/C in HeLa cells is mediated by a complex of BUBR1, BUB3, CDC20, and MAD2. *J Cell Biol* 154: 925-936.

• Sullivan M, Morgan DO (2007). Finishing mitosis, one step at a time. *Nat Rev Mol Cell Biol* 8: 894-903.

• Tanaka TU, Desai A (2007). Kinetochore-microtubule interactions: the means to the end. *Current Opinion in Cell Biology* 19: 1-11.

• Taylor SS, Scott MI, Holland AJ (2004). The spindle checkpoint: a quality control mechanism which ensures accurate chromosome segregation. *Chromosome Res* 12: 599-616.

• Tighe A, Johnson VL, Albertella M, Taylor SS (2001). Aneuploid colon cancer cells have a robust spindle checkpoint. *EMBO Rep* 2(7): 609-614.

• Toyota M, Sasaki Y, Satoh A, Ogi K, Kikuchi T, Susuki H, Mita H, Tanaka N, Itoh F, Issa J-PJ, Jair K-W, Schuebel KE, Imai K, Tokino T (2003). Epigenetic inactivation of CHFR in human tumours. *Proc Natl Acad Sci* 100(13): 7818-7823.

• Uziel T, Zindy F, Sherr CJ, Roussel MF (2006). The CDK inhibitor $p18^{Ink4c}$ is a tumour suppressor in medulloblastoma. *Cell Cycle* 5(4): 363-365.

• van den Heuvel S (2005). Cell-cycle regulation, *WormBook*, ed. The *C. elegans* Research Community, WormBook, doi/10.1895/wormbook.1.28.1

• Vermeulen K, Van Bockstaele DR, Berneman ZN (2003). The cell cycle: a review of regulation, deregulation and therapeutic targets in cancer. *Cell Prolif* 36: 131-149.

• von Bueren AO, Shalaby T, Rajtarova J, Stearns D, Eberhart CG, Helson L, Arcaro A, Grotzer MA (2007). Anti-proliferative activity of the quassinoid NBT-272 in childhood medulloblastoma cells. *BMC Cancer* 7:19.

◆ Wang Y, Burke DJ (1995). Checkpoint genes required to delay cell division in response to nocodazole respond to impaired kinetochore function in the yeast *Saccharomyces cerevisiae. Mol Cell Biol* 15: 6838-6844.

◆ Weaver BA, Cleveland DW (2005). Decoding the links between mitosis, cancer, and chemotherapy: The mitotic checkpoint, adaptation, and cell death. *Cancer Cell* 8(1): 7-12.

◆ Wechsler-Reya RJ (2003). Analysis of gene expression in the normal and malignant cerebellum. *Recent Progress in Hormone Research* 58: 227-248.

◆ Winey M, Huneycutt BJ (2002). Centrosomes and checkpoints: the MPS1 family of kinases. *Oncogene* 21: 6161-6169.

◆ Yang Z, Lončarek J, Khodjakov A, Rieder CL (2008). Extra centrosomes and/or chromosomes prolong mitosis in human cells. *Nature Cell Biology* 10(6): 748-751.

◆ Yazigi-Rivard L, Masserot C, Lachenaud J, Diebold-Pressac I, Aprahamian A, Avran D, Doz F (2008). Childhood medulloblastoma. *Arch Pediatr* 15(12): 1794-1804.

◆ Yuan B, Xu Y, Woo J-H, Wang Y, Bae YK, Yoon D-S, Wersto RP, Tully E, Wilsbach K, Gabrielson E (2006). Increased expression of mitotic checkpoint genes in breast cancer cells with chromosomal instability. *Clin Cancer Res* 12(2): 405-410.

◆ Zhou J, Panda D, Landen JW, Wilson L, Joshi HC (2002). Minor alteration of microtubule dynamics causes loss of tension across kinetochore pairs and activates the spindle checkpoint. *J Biol Chem* 277: 17200-17208.